

Louisiana State University LSU Digital Commons

LSU Doctoral Dissertations

Graduate School

2010

The weakening of branch predictor performance as an inevitable side effect of exploiting control independence

Christopher Joseph Michael

Louisiana State University and Agricultural and Mechanical College

Follow this and additional works at: https://digitalcommons.lsu.edu/gradschool_dissertations



Part of the [Electrical and Computer Engineering Commons](#)

Recommended Citation

Michael, Christopher Joseph, "The weakening of branch predictor performance as an inevitable side effect of exploiting control independence" (2010). *LSU Doctoral Dissertations*. 1856.

https://digitalcommons.lsu.edu/gradschool_dissertations/1856

This Dissertation is brought to you for free and open access by the Graduate School at LSU Digital Commons. It has been accepted for inclusion in LSU Doctoral Dissertations by an authorized graduate school editor of LSU Digital Commons. For more information, please contact gradetd@lsu.edu.

THE WEAKENING OF BRANCH PREDICTOR PERFORMANCE
AS AN INEVITABLE SIDE EFFECT
OF EXPLOITING CONTROL INDEPENDENCE

A Dissertation
Submitted to the Graduate Faculty of the
Louisiana State University and
Agricultural and Mechanical College
in partial fulfillment of the
requirements for the degree of
Doctor in Philosophy

in

The Department of Electrical and Computer Engineering

by
Christopher J. Michael
B.S. Louisiana State University 2005,
May 2010

Acknowledgments

There are several people whom I would like to thank for their time and effort in helping me throughout my time conducting this research.

To my major professor, Dr. David M. Koppelman, thank you for the outstanding technical guidance you have given me in the many years I have conducted this research. Also, for sparking my interest in computer architecture through your wonderful teaching.

A big thanks to my minor professor, Dr. Thomas Sterling. The guidance and advice you have given me in the past several years are invaluable. It has been an honor working with you.

Thanks to all other members of my committee for your time and teaching. Dr. J. (Ram) Ramanujam, Dr. Lu Peng, Dr. Jerry Trahan, and Dr. Joseph Giaime, I was very fortunate to be taught by each of you in my many years here at LSU.

My time in graduate school would be much more of a struggle if it wasn't for the many friends I have made here. You know who you are. Thank you.

Finally, I must thank my family both present and future. You all were very patient in dealing with all my time away.

Especially my future wife, Meg, whom I am scheduled to marry the day this dissertation is due. Thanks for putting up with me in this hectic time.

Table of Contents

Acknowledgments	ii
List of Tables	v
List of Figures	vi
Abstract	viii
1 Introduction	1
2 Background	7
2.1 Branch Prediction	7
2.1.1 Common Predictors	8
2.1.2 Correct and Timely History Update	12
2.2 Paths	13
2.3 Branch Behavior	15
2.4 Branch Overlap and Update Lag	18
3 Control Independence	21
3.1 Implementation Issues	22
3.1.1 CD- or CI-First	22
3.1.2 Register Remapping and Speculative Execution	22
3.1.3 Finding the Reconvergence Point	24
3.1.4 Selective Squashing	25
3.1.5 Targeting Branches That Are Difficult to Predict	26
3.1.6 Areas of Low Potential for Benefit	27
3.2 Snipper	27
4 Prior Work	32
4.1 Limit Studies	32
4.2 Branch Classification and Prediction Techniques	33
4.3 Early Control Independence Processors	36
4.3.1 Multiscalar	36
4.3.2 Dynamic Control Independence	37
4.3.3 Skipper	37
4.4 Transparent Control Independence	38
4.5 Ginger	39
5 System Simulation Methodology	41
5.1 Simulation Software	41
5.2 Configuration of Simulated System	42
5.3 Selected Branch Predictors	45
5.4 Benchmarks	47

5.5	Viewable Experimental Data	48
6	Branch Weakening	50
6.1	The Broad Classes of Weakening	50
6.2	Prevalence of Weakening Types	55
6.3	Mangled-Update Weakening	56
6.3.1	Description	56
6.3.2	Example	58
6.3.3	The Effect of Delayed Update on Branch Prediction Accuracy	58
6.3.4	Reducing Mangled-Update Weakening	63
6.3.5	Flexible Update Schemes	67
6.3.6	Performance of Flexible Update Schemes	69
6.4	Mangled-Path Weakening	72
6.4.1	Description	72
6.4.2	Examples	73
6.4.3	Path Splitting and Joining	75
6.4.4	The Effect of Path Splitting and Path Joining	82
6.4.5	Outcome History Padding	84
6.5	Performance of Outcome History Padding Schemes	87
7	Measurement by Weakening Type	91
7.1	Approach	91
7.2	Model Systems	92
7.3	Results	94
8	CI Aware Branch Predictor	97
8.1	Implementation	97
8.2	Results	98
9	Conclusion and Future Work	102
	Bibliography	105
	Vita	109

List of Tables

2.1	Branch Behavior Definitions	14
5.1	Configuration Parameters	43
5.2	Selected Benchmarks	48
6.1	Branch Weakening Types	54
6.2	Padding Methods	87

List of Figures

1.1	Sample Code and Control Flow Graph	3
1.2	Fetch Stream Comparison	4
2.1	Classification of Branches and 16-bit Paths	17
2.2	Example of Overlap	19
3.1	Snippet Speedup	30
5.1	Static Snippet vs. Dynamic Snippet, Speedup and Weakening	44
5.2	Branch Predictors Used in this Study	46
6.1	Snippet Weakening	51
6.2	Example Control Flow of Execution	52
6.3	Weakening Classified by Type for Snippet	55
6.4	Example of Delayed Update Weakening	57
6.5	The Impact of Update Lag	59
6.6	Update Lag Induced by Snippet	61
6.7	The Behavior of Predictor Update Schemes for a Vacillating Branch	63
6.8	Markov Model of Predictor Entry State	64
6.9	Overlap and Vacillation for Snippet	66
6.10	Misprediction Rate Impact of Flexible Update Schemes	69
6.11	Analysis of Bimodal Chooser	70
6.12	GHR State for Branch 0x12fbc	74
6.13	Control Flow Graphs of Two Separate Executions	74
6.14	Examples of Path Splitting and Joining	77
6.15	Examples of External Insulated Weakening	78
6.16	Push Displacement Causing Path Joining	79
6.17	Control Flow Example for CDR Juggling	80
6.18	Static Path Rate for Several Systems	81

6.19	Misprediction Rate And Collision Impact of Padding Schemes for GShare	88
6.20	Misprediction Rate And Collision Impact of Padding Schemes for Hybrid	89
7.1	Weakening Among Model Systems	95
8.1	Performance of Hybrid CIAP	98
8.2	Weakening Classified by Type for Snipper with CIAP	100

Abstract

Many algorithms are inherently sequential and hard to explicitly parallelize. Cores designed to aggressively handle these problems exhibit deeper pipelines and wider fetch widths to exploit instruction-level parallelism via out-of-order execution. As these parameters increase, so does the amount of instructions fetched along an incorrect path when a branch is mispredicted. Many of the instructions squashed after a branch are control independent, meaning they will be fetched regardless of whether the candidate branch is taken or not. There has been much research in retaining these control independent instructions on misprediction of the candidate branch. This research shows that there is potential for exploiting control independence since under favorable circumstances many benchmarks can exhibit 30% or more speedup. Though these control independent processors are meant to lessen the damage of misprediction, an inherent side-effect of fetching out of order, branch weakening, keeps realized speedup from reaching its potential. This thesis introduces, formally defines, and identifies the types of branch weakening. Useful information is provided to develop techniques that may reduce weakening. A classification is provided that measures each type of weakening to help better determine potential speedup of control independence processors.

Experimentation shows that certain applications suffer greatly from weakening. Total branch mispredictions increase by 30% in several cases. Analysis has revealed two broad causes of weakening: changes in branch predictor update times and changes in the outcome history used by branch predictors. Each of these broad causes are classified into more specific causes, one of which is due to the loss of nearby correlation data and cannot be avoided. The classification technique presented in this study measures that 45% of the weakening in the selected SPEC CPU

2000 benchmarks are of this type while 40% involve other changes in outcome history. The remaining 15% is caused by changes in predictor update times. In applying fundamental techniques that reduce weakening, the Control Independence Aware Branch Predictor is developed. This predictor reduces weakening for the majority of chosen benchmarks. In doing so, a control independence processor, *snipper*, to attain significantly higher speedup for 10 out of 15 studied benchmarks.

Chapter 1

Introduction

Processors designed to exploit instruction-level parallelism (ILP) via out-of-order execution require long pipelines and high fetch rates. As these parameters increase, so does the amount of instructions fetched along an incorrect path when a branch is mispredicted. In runs of selected applications in the SPEC CPU 2000 benchmark suite [Hen00]. On a CPU with a modern configuration, around 30% of fetch bandwidth is taken by instructions that will eventually be squashed. Some of these instructions will be fetched regardless of the direction of a branch. In current conventional systems, these *control independent* instructions are always squashed upon branch misprediction and are fetched again shortly thereafter. Recent research efforts explore lessening the effect of branch mispredictions by retaining these instructions when squashing [AZRRA07, HR07, SBV95] or fetching them in advance when encountering a branch that is difficult to predict [CV01]. Though these *control-independent processors* (CIPs) are meant to lessen the damage of misprediction, an inherent side-effect of fetching out of order, *branch weakening*, keeps realized speedup from reaching its potential. The goal of this study is to formally define and analyze the different causes of branch weakening, measure the effect of each, and offer many techniques to help relieve CIPs of weakening. It will be shown that some weakening is unavoidable. Several different types of weakening will be quantified and, in doing so, the amount of unavoidable weakening is realized. This further validates the feasibility of exploiting control independence.

Modern general purpose processors are designed to minimize execution times by allowing for

high clock rates. This is made possible by pipelining the several stages of instruction execution, from when the instruction is first fetched to the time it commits. In addition, the processor is made *superscalar*, meaning it can sustain execution of multiple instructions per cycle. These types of processors must predict branches to maintain pipeline efficiency. When a branch instruction is fetched, the direction of the branch will not be known until several cycles and many instructions later. Accurate branch prediction is crucial to conventional processor cores. The *instruction window size*, or the maximum number of instructions a processor may have executing at any time, directly determines the potential waste fetching *doomed instructions*, which will eventually be squashed because a branch is mispredicted. CIPs lessen the impact of branch misprediction by retaining otherwise doomed instructions that will immediately be re-fetched after the squash.

Many studies have shown that reasonable CIP implementations can yield high gains. The Transparent Control Independence implementation by Al-Zawawi et al. achieves an average speedup of 22% across 15 SPEC CPU benchmarks [AZRRA07]. Another recent CIP, Ginger, developed by Hilton and Roth, achieves an average speedup of about 5% but does so with a much less aggressive predictor [HR07]. Both of these CIPs are affected by significant amounts of branch weakening.

Branch predictors of conventional processors often use a *global history register* (GHR) to correlate on recent outcomes and attain high branch prediction accuracy. The GHR is simply a bitwise shift register that holds the *global history*, a set number of recent consecutive branch outcomes. Outcomes in a conventional system's GHR may be guaranteed to be true; however, outcomes in the GHR may be incorrect or missing in a CIP.

Branch weakening is caused by incorrect or missing history data in the GHR and changes to

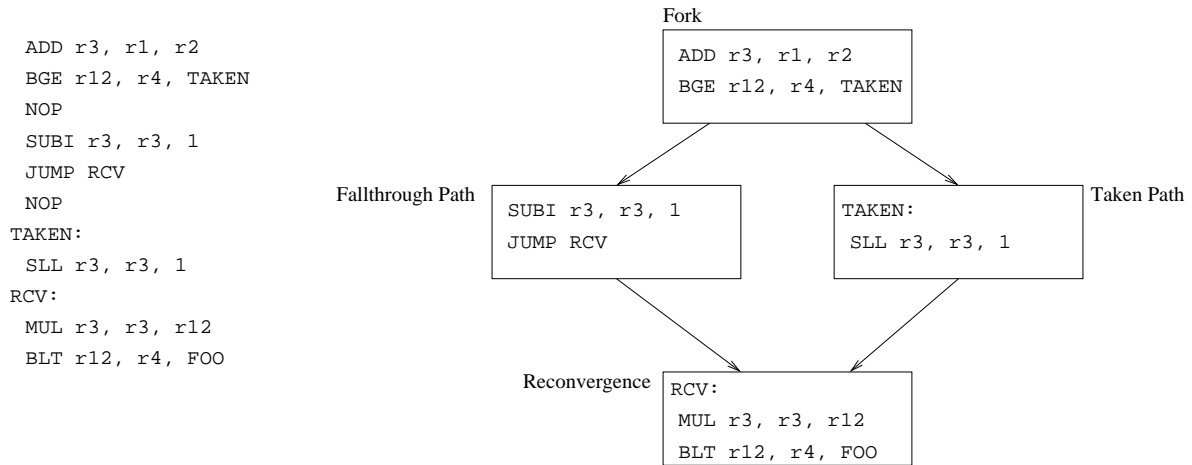


Figure 1.1: Sample Code and Control Flow Graph

the way in which branch predictors are updated.

Figure 1.1 shows a snippet of code along with a control-flow diagram describing the possible paths of execution. Assume branch BGE is difficult to predict. When this branch is fetched in a conventional system, an initial prediction of its outcome is made and fetching continues along the predicted path. By the time BGE resolves, instructions far beyond the block labeled **reconvergence** have been fetched. If the branch is resolved mispredicted, all instructions after the branch are squashed and fetching continues along the correct path from the branch. Note that most instructions that were squashed will be refetched once again, this time along the correct path. For typical aggressive dynamically scheduled systems running applications like those in the SPEC CPU 2000 set, nearly 80% of the total instructions squashed upon misprediction of a branch like BGE will be fetched again soon after. The flushing and refetching of these instructions costs energy and time, since the instructions will have to be decoded and issued again.

Now consider a CIP executing the code fragment that chooses to exploit control independence for the branch BGE. First, the **fork**, **taken path**, and then **reconvergence** region may be fetched in order, similar to a conventional system. When BGE resolves as mispredicted, the CIP will squash

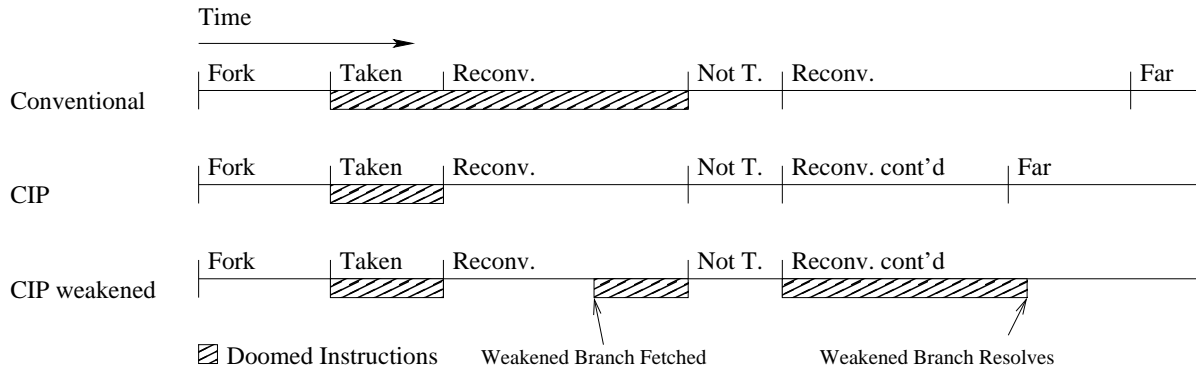


Figure 1.2: Fetch Stream Comparison

only the **taken path** region and fetch the **fallthrough path** retaining all control independent instructions in the pipeline while recovering from the branch misprediction. After **fallthrough path** is completely fetched, fetching will continue where it left off when BGE resolved mispredicted.

A CIP will speed this execution because fetch bandwidth is not wasted by squashing and refetching the instructions in the reconvergence region and beyond, as shown in Figure 1.2. The highlighted regions in the figure indicate the fetching of doomed instructions. Notice that in the conventional case, the **reconvergence** region is squashed and later refetched. The second diagram shows what would ideally happen in a CIP. Because there is less time spent fetching doomed instructions, some subsequent region of code **far** is fetched sooner than in the conventional case. In the third diagram, the impact of weakening is shown. Some branch in the **reconvergence** region, which would not be mispredicted in the conventional case, is mispredicted in the CIP. As a result, the system fetches considerably more doomed instructions. In this case, weakening has caused control independence exploitation to slow execution down rather than speed it up. Comparing the diagrams of the conventional system and the weakened CIP, it is evident that more of the fetch bandwidth is wasted on doomed instructions in the weakened case. It becomes clear that to exploit control independence as much as possible, there should be some action taken

to minimize negative effects caused by branch weakening.

Weakening is caused by two broad reasons. The increase of in-flight instructions and the prolonged commit times of branches in a CIP cause predictors to be updated differently than they would in a conventional system. Additionally, if predictors in the conventional system update earlier than commit time, the additional speculative execution required by a CIP could induce incorrect predictor updates. This type of weakening involving predictor update times may be avoided through techniques that selectively update the predictor earlier than the time at which branches commit. The other broad cause of weakening is caused by incorrect or missing branch outcomes in the GHR of CIPs. This property either introduces useless outcomes into the outcome history, called *noise ingestion*, or robs the history of important correlation data, called *signal loss*. The term *noise* refers to a branch outcome that varies in the GHR that isn't correlated to any branch which uses it for prediction. Noise ingestion causes branches in a CIP to be associated with more table entries in the predictor. Each of these extra entries will need to be trained and the mispredictions due to this cause weakening. Weakening due to noise ingestion can be alleviated with outcome history update methods that reduce the amount of unnecessary outcomes brought in to the GHR when exploiting control independence. The term *signal* refers to a branch outcome in the GHR that is useful for correlation of branches that use it. When branches are weakened due to signal loss, the more common case is that the weakening cannot be avoided since the correct outcomes cannot possibly be determined. This type of weakening cannot be reduced. In other less likely cases the signal is discarded as a side effect of fetching out of order which can be avoided by careful GHR management.

If weakened branches are classified into the reasons just presented, then the amount of avoid-

able weakening may be measured. The goals of this study are as follows. First, to develop definitions, identify characteristics, and quantify the major types of weakening. This includes a full analysis of the CIP artifacts that cause each type of weakening. Second, to provide an understanding of how each type of preventable weakening may be avoided while providing insight towards how much weakening is inevitable. The final goal is to develop techniques to lessen the effects that cause weakening using a fundamental approach brought about by achieving the prior goal.

Chapter 2

Background

2.1 Branch Prediction

In early pipelined single-issue processors, branches could resolve one cycle after being fetched. Instead of leaving a bubble of inactivity in the pipeline, every branch had a subsequent *delay slot* instruction that would be executed independent of the branch's path. Since correct branch outcomes were usually available when needed, no branch predictor was necessary. Current generation superscalar processors fetch many instructions per cycle and contain many more pipeline stages [Sit93, Sto06, Sto01, TDF⁺02]. This greatly enlarges the potential bubble, making delay slots unreasonable and branch prediction vital.

A *basic block* is a sequence of code in which execution always starts with its first instruction and ends with its last instruction with no branching in between. A basic block contains at most one branch instruction and this instruction must be at the end of the basic block. A *branch* is an instruction that usually¹ tests a condition to control the flow of instructions. A branch can either be *taken*, denoted *T*, or *not taken*, denoted *N*, and this is referred to as the branch's *direction*. If a branch is not taken, then the instruction in the program that comes after the branch is fetched. If taken, then control flow changes to some destination address specified by the branch instruction. A *static branch* is an instruction in code that resides in some memory location. Fetching a static branch creates a *dynamic branch*. A dynamic branch is said to be *in-flight* from the time it is fetched to the time it has been committed or squashed. Multiple in-flight dynamic branches may correspond to a single static branch. A *branch predictor* is an architectural component in

¹Some instruction set architectures contain branches that are always taken.

the processor that tries to determine the direction of a branch in order to increase instruction throughput. The *branch target buffer* is a component that tries to provide the target of a taken branch before it is computed later in the pipeline. A dynamic branch is said to *resolve* in the cycle that its condition is tested. If the branch is mispredicted, the CPU must perform a *recovery* by squashing all instructions after the mispredicted branch and resuming fetch along the correct path of the branch. At some point after a branch's resolve time, it updates its predictor entry to reflect its direction. This occasion is simply referred to as branch *update*. Further detail regarding the fundamentals of branch prediction and other modern computer architecture concepts can be found in the Hennessey and Patterson texts [HP03, HP08].

The metrics used to measure the performance of branch predictors are the *branch prediction ratio* and the *branch misprediction rate*. The branch prediction ratio is the number of correct predictions divided by the total number of predictions of some defined execution. The branch misprediction rate is the number of branch mispredictions divided by a given rate of instructions. Branch prediction ratios and branch misprediction rates in this study are always measured for only committed branches. The misprediction rates are measured in mispredictions per 1000 committed instructions, denoted $misp/kI$.

There are special prediction techniques for *indirect branches*, those that branch to a target specified by a register. The address to which these instructions branch may change throughout execution. These types of predictors are not considered in this study.

2.1.1 Common Predictors

Simple predictors, such as the that in the ARM810 processor [ARM], implement *static branch prediction* schemes. In these schemes, prediction is based on the static branch and is used for

all dynamic instances of that branch. More modern predictors such as the Pentium 4 use a static predictor while the system's more complex predictor is training [Sto01]. The static predictors in these architectures predict all forward branches (branches whose target is further in code) not taken while all backwards branches are predicted taken. This is intuitive, since most backwards branches belong to loops and are expected to be taken most of the time. In an early study by James E. Smith, the need for *dynamic branch prediction* was addressed [Smi81]. Dynamic branch prediction schemes predict branches based on program run-time characteristics. For example, a branch may be predicted as its last resolved outcome in a program. The Smith study shows that on average about 4% improvement in branch prediction accuracy for a small set of benchmarks can be attained using this very simple method over a static scheme where branches are predicted based on their operation codes. More advanced dynamic predictors discussed in the remainder of this section can drastically improve basic static schemes, increasing the branch prediction ratio by 40% in some cases.

The bimodal predictor [Smi81] is a popular and relatively simple dynamic branch predictor. It is a *per-address branch predictor*, meaning it indexes a *branch history table* (BHT) using the address of the branch it is predicting. Each BHT entry consists of a 2-bit saturating up-down counter. Note that though some predictors may implement some other finite automaton for their table entries, all predictors in this study use an up-down counter. The most significant bit of the counter indicates the prediction of the branch. In this study, it is assumed that the branch will be predicted not taken if this bit is 0 while the branch is predicted taken if this bit is 1. Upon predictor update, the counter will be incremented or decremented based on the branch's correctly resolved direction. A not-taken outcome will decrement the entry while a taken outcome will

increment it.

More advanced dynamic branch prediction techniques use two levels of branch history. Tse-Yu Yeh and Yale N. Patt studied and compared some variations of two-level predictors [YP92]. These predictors were both per-address and *correlating*, meaning that some type of outcome history data is used to make each prediction. The GAg predictor described in the study is an example of a correlating predictor. A special register, named the *global history register* or GHR, keeps a record of the last k outcomes of branches that executed. At predict time, the GHR is used to index a *pattern history table*, or PHT, of saturating counters and a prediction is made using the counter's value. Once the branch's outcome is known, this entry is updated appropriately. This predictor is named GAg to stand for Global Address, global PHT.

The best performing predictor in the study is the PAg predictor (per-address, global PHT). A first table is indexed by a branch's address and contains the *local history* for the branch. This is the sequence of outcomes for the last k instances of the static branch. The local history will then index a global PHT that contains a saturating counter used for prediction. The study showed on a whole that various dynamic two-level branch predictors yield a 97% accuracy on average for various SPEC92 CPU benchmarks.

In a study by Scott McFarling in 1993, the GShare predictor is introduced [McF93]. GShare is a two-level predictor whose global and per-address information are shared in the first level by XORing the PC and global history. This value indexes a PHT of saturating counters that yields the prediction. This is a popular and well performing predictor, averaging near 97% accuracy under selected benchmarks with a 32kiB table. An important technique introduced by McFarling in this study is the combining of branch predictors to form a *hybrid* predictor. This type of predictor is

built to select the better prediction option of any two predictors. It uses a *chooser* table, which is a per address table of two-bit saturating counters. On a branch prediction, the chooser will select either of the two predictors. On update, if one and only one of the predictors mispredicted, the chooser entry will be updated towards choosing the one that is correct. A 32kB bimodal/GShare Hybrid predictor outperforms a 32kB GShare predictor in every benchmark selected for the study.

There are many other predictors that correlate on some form of global history [EM98, YP93]. Some predictors, such as the perceptron predictor [JL01], are much more advanced than ones described here. Though these predictors are valuable, their complexity makes them less practical for study. Due to its ease of understanding, GShare is the only correlating predictor (or predictor component) that will be used in this study.

Numerous current-generation processors use correlating predictors to improve performance. One example is Intel's Core processor which was designed with a relatively more complex predictor than others implemented at the time [Sto06]. The branch predictor has a type of bimodal/global hybrid component similar to the hybrid predictor used in this study. The predictor also has a special *loop detector* component that predicts when loops will terminate. The architecture also implements an indirect branch predictor.

Another example of a modern processor that uses a correlating predictor is the IBM POWER4 architecture [TDF⁺02]. It also has a similar type of hybrid predictor. The per-branch component, called a *local predictor*, is a 16k-entry BHT consisting of 1-bit entries. The correlating predictor component, called a *global predictor*, uses an 11-bit vector, much like a GHR, called a *global history vector*. This register is XORed with the PC to index a *global history table* of 1-bit entries. The chooser component, called the *sector table*, is also a table of 1-bit entries but, unlike GShare,

it is indexed in the same manner as the global history table.

2.1.2 Correct and Timely History Update

A *wrong path history update* occurs when a doomed branch updates the branch predictor. The effects of wrong path history updates have been presented by Jourdan et al. [JSHP97]. In the study, several predictors, GShare being one of them, updating outcome history at predict time are compared to their counterparts that update non-speculatively at commit time. Several mechanisms are covered that enable speculatively updating history at branch predict time while assuring that the history is correct. It is shown that performance drops by 30% on average if speculative global histories are not repaired across the proposed techniques. The predictor component that causes most of this degradation is the GHR. This suggests that some checkpointing mechanism that repairs the GHR on a misprediction is vital to the predictor. Because branches may resolve out of order, a PHT entry may be erroneously updated if predictors are set to update at resolve time (for example, when a doomed branch resolves). The study reveals that this speculative updating of the PHT without repair has almost no effect on performance. However, a BHT may be more vulnerable to incorrect updates since instances of the same branch tend to appear closer together in execution compared to instances of the branch reached by same path.

Branch predictors that have long prediction latencies either cause the CPU clock to have a lower frequency or require a pipelined implementation of the predictor. Pipelined predictor implementations leave bubbles in the instruction pipeline, decreasing the fetch rate. Daniel A. Jiménez et al. establish that it is not enough for a predictor to attain a higher accuracy, it must also provide a timely prediction [JKL00]. One technique offered in the study to improve the performance of systems with more complex predictors is *overriding*: Using a smaller and faster

predictor to make an initial 1-cycle prediction while waiting for more accurate prediction from a larger more complex predictor. A study by Gabriel H. Loh explores, in addition to prediction latencies, that predictor update latencies are also a significant factor of performance degradation – especially on deeply pipelined (40-stage) systems [Loh06]. The study shows that when using an overriding predictor the more complex component, in this case perceptron, can be used to provide a quick (though perhaps incorrect) update to the smaller 1-cycle component, GShare, to attain about 5% speedup in IPC for selected SPEC CPU benchmarks on a 40-stage pipelined system. This technique is called *hierarchical update*. It is claimed that update latency of highly accurate predictors are only affected by update latency in the initial training phase of the predictor, while smaller predictors are much more vulnerable due to their size.

2.2 Paths

For a correlating predictor, entries in the predictor’s PHT correspond to paths by which the predicted branch was reached. In this study, the term *path* is the PHT index used when predicting a dynamic instance of a branch. The branch is said to be *reached by* the path. The GShare predictor used in this study constructs its path by XORing a k -outcome GHR to k bits of the branch PC.

Define the *true path* as the path reached by a non-doomed instruction in a conventional system that maintains a correct GHR and computes the path as defined by the predictor. A *pure path* of a branch is a sequence of the last k correct global outcomes in program order (equivalently, the contents of a k -bit GHR on a conventional system). Any path observed by a non-doomed instruction is referred to as an *observed path*. It will be shown further in the study that observed paths may not always be true paths in a CIP.

The *path filtered local history* of a static branch for some given path is the local history for

Table 2.1: Branch Behavior Definitions		
Name	Definition	Example
Mono-	$M_0(B) \leq M_1(B)$	
Monostable	$M_0(B) = 0$	TTTTTTTTTTTTTT
Monoloop	$M_2(B) = 2M_1(B)$	TTTNTTTTTNTTT
Mono-other	All other mono-	
Bi-	$M_1(B) < M_0(B)$	
Bistable	$M_1(B) < M_2(B)$	NNNNTTNTNTTTT
Bibiased	$M_2(B) = 2M_1(B)$	TTTTTTNNNNNNN
Other	All other behavior	

that branch which only includes outcomes of the branch reached by that path. Path filtered local history is used to study branch outcomes relevant to correlating predictors.

Because many branches may share PHT or BHT entries, branch predictors are subject to *collisions* which hurt branch prediction accuracy. A collision occurs when a branch uses some predictor entry it had previously updated but had since been updated by some other branch.

If every path of every branch had its own PHT entry, the pattern index computed using a simple hashing would have to be $k + b$ bits long, where 2^b is the maximum number of static branch instructions allowed. For some reasonable k , the size of this PHT would be wildly impractical. This is the reason *outcome history hashing* is used to generate a reasonably sized path. Call an *optimal outcome history hash* one that yields the highest branch prediction accuracy for a given PHT size. The GHR XOR PC hash of the GShare predictor is a sound approach since it enables the path to be influenced by both the static branch and the global history. However, there may be better outcome history hashing allowing for accuracies closer to the optimal. Understanding branch behaviors may allow for better hashing techniques, but analyzing it out of the context of weakening is beyond the scope of this study.

2.3 Branch Behavior

There are several behaviors exhibited commonly by branches. Classification of branches by their behavior helps bring about understanding as to how branches are weakened. Define B as the full outcome sequence of some static branch. Let $M_0(B)$ denote the number of times B is mispredicted when using a *perfect static predictor*. A perfect static predictor has prior knowledge of the most frequent direction in B and always predicts the branch in that direction. Let $M_1(B)$ and $M_2(B)$ denote the number of times a dynamic bimodal predictor mispredicts the branch with a 1-bit saturating counter and 2-bit saturating counter, respectively.

The definitions of several branch behaviors are given in Table 2.1. Branches that favor a static prediction are named with the prefix *mono-* while those that prefer dynamic prediction are named with *bi-*. Typically in literature, the term *biased* is used to describe what is referred to here as monostable behavior when B contains all taken or all not-taken outcomes. The monoloop behavior is typically referred to as just a *loop* behavior, when B contains all similar outcomes separated by single opposing outcomes. Monostable and monoloop branches are predicted accurately with a bimodal predictor. Monoloop branches are predicted best with a 2-bit saturating counter, since using a 1-bit saturating counter causes an extra misprediction of the branch after every loop exit. This may be in part the reason why most branch predictors employ 2-bit counters as opposed to other sizes. Two mono- branches are called *unanimous* if their favored outcomes are in the same direction. The branches are said to be *dissonant* if their outcomes are in opposing directions.

Bistable and bibiased branches exhibit long *runs* of the same outcome, where a run is a subsequence of similar outcomes for a branch. A branch classified as bibiased has only large runs in its outcome history, therefore a predictor with a 1-bit saturating counter will yield half the mis-

predictions of a predictor with a 2-bit counter. The bistable class allows for a little more leniency. Branches can be classified this way if they are more accurately predicted with a predictor using a 1-bit saturating counter than one using a 2-bit saturating counter. Recall that for both of these behaviors, a 1-bit saturating counter outperforms a perfect static predictor.

Though the definitions above specifically refer to the behavior of a branch's local history, they apply to path filtered local histories as well. The implications of each static branch's local history behavior on a per-address predictor such as bimodal carry on to the branch's path filtered local histories on a correlating predictor. For the remainder of the section, branch local histories will be used to describe behaviors, but path filtered local histories apply as well.

The plot in Figure 2.1 shows the measurement of branch behaviors as defined above for branches and 16-bit paths. Paths are constructed by XORing the 16 bits of the branch's PC with 16 bits of the global history, similarly to the way GShare constructs paths. Results are shown as percentages of dynamic branches. The benchmarks are those selected for this study and will be presented in detail later in Section 5.1 along with RSIML, the simulator used to collect results. These results are taken directly from RSIML output, which includes the classification in its distribution. Results are gathered via functional simulation. The way in which the classification is performed will now be discussed briefly.

The module of RSIML that classifies branches and path filtered local histories assigns a pre-defined class to each branch or path by using the branch prediction accuracies of a set of n i -bit saturating counter predictors. The counter predictors for each branch or path are incremented if taken and decremented if not taken. The most significant bit of the counter is used to make a prediction. If the first outcome of the branch or path is T, the counter is set to its maximum

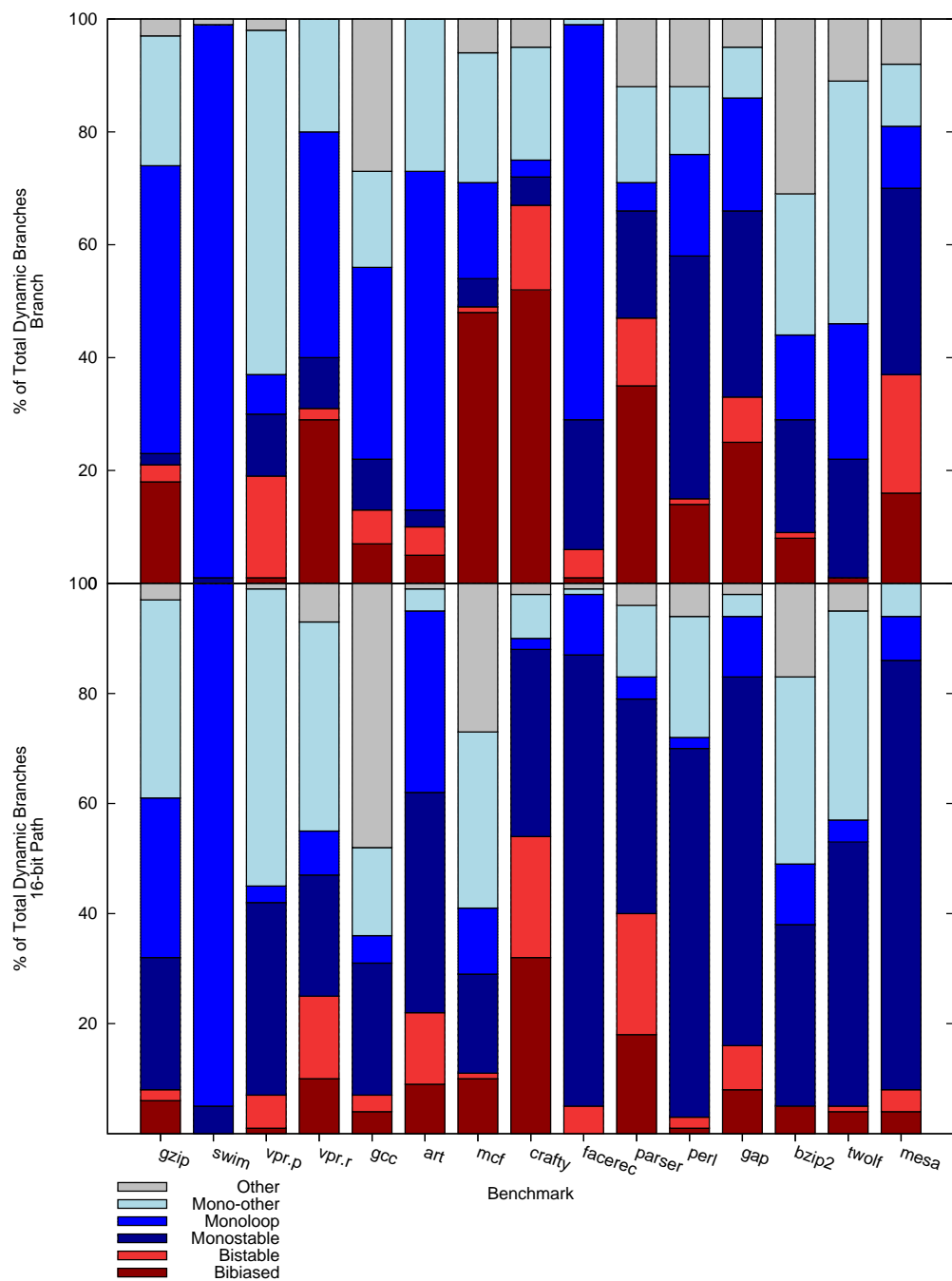


Figure 2.1: Classification of Branches and 16-bit Paths (petdis.134, functional simulation)

value. If N, it is set to zero. Predictors of size 1 to 6 bits are used and in addition the total number of taken outcomes is tallied. Let $M_i(B)$ denote the number of mispredictions of an i -bit counter predictor. $M_0(B)$ is a special case that denotes the number of the less common outcome in the local history of a branch (this is the number of mispredictions yielded by a perfect static predictor). Let $M_m(B)$ be the minimum number $M_i(B)$ for all i from 0 to n . Branches are then classified in the following order.

Monostable if $M_0(B) = 0$; else,

Monoloop if $M_0(B) - M_1(B)/2 < 2$; else,

Mono-Other if $M_0(B) \leq M_m(B)$; else,

Bistable if $M_2(B) > M_1(B)$; else,

Bibiased if $M_m(B) > 1.01M_0(B)$; else,

Other

Referring back to Figure 2.1, note that many of the benchmarks have significant amounts of bistable and bibiased branch and path behaviors. Branches of these types certainly prefer a speedy predictor update and suffer more training mispredictions, as will be explained in more detail further in the study when discussing weakening.

2.4 Branch Overlap and Update Lag

Branch *overlap* becomes important when studying weakening dealing with predictor update. A branch is said to overlap if one dynamic instance of the branch is predicted before a prior non-doomed instance of the same branch updates its predictor entry. This behavior is usually exhibited in tight loops when the system is executing many instances of a small group of static instructions. A path is said to overlap if one instance of the path is predicted before a prior non-doomed instance of the same path updates its predictor entry. This is referred to as *path overlap*.

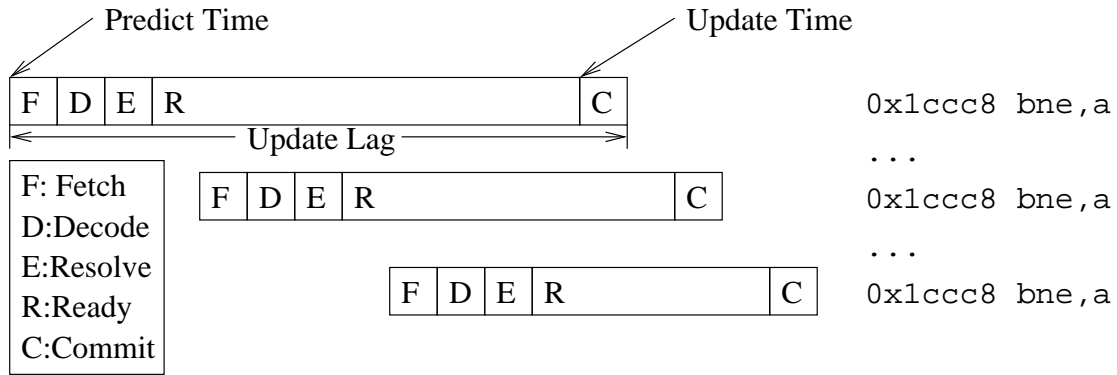


Figure 2.2: Example of overlap taken from the bzip2 benchmark

Call the time from when a dynamic branch is predicted to the time the predictor is updated the *update lag*. Update lag can be measured in many ways. Call the *cycle update lag* the number of cycles from predict to update of a branch. Call the *instruction update lag* the number of instructions fetched from predict to update of a branch. The *branch update lag* is the number of branches fetched from predict to update of a branch.

There are cases in which conventional systems are sensitive to update lag. An overlapping branch is shown in the pipeline execution diagram of Figure 2.2 with the update lag for the first instance marked. Assume this branch to be a simple if-then-else statement within some loop body. Other instructions and all squashed instances of the branch have been removed for clarity. Assume the branch to be bistable. The first instance shown represents the beginning of a run. When this instance resolves, it squashes all subsequent instructions and fetches along the correct path (The instance does not commit right after resolving due to out-of-order execution). Notice that all other instances shown in the figure are fetched along the correct path, but do not see the update of the first instance. All the instances will mispredict. If the update lag were decreased by setting the predictor to update at resolve time, each instance will see all prior updates. The reduction of update lag causes the third instance to be predicted correctly. Situations like these

do not occur too often in conventional systems because branches usually commit soon after they resolve. It will be shown further in the study that lag and overlap are more relevant in a CIP.

Intuitively, branch overlap is expected to happen more frequently than path overlap. This is because when two instances of a static branch overlap, their paths may be different. Even so, there may still be plenty of path overlap in execution. This will be revisited and elaborated with data further in the study.

Chapter 3

Control Independence

A non-doomed dynamic instruction is control independent (CI) of a candidate dynamic branch if it is fetched regardless of the direction of the candidate [LW92]. Instructions are control dependent (CD) if they are fetched on only one direction of the candidate.

Refer back to Figure 1.1. Recall that branch BGE is a difficult branch to predict, so the CIP may *protect* it, exploiting control independence so that fewer instructions are squashed when it is mispredicted. Branch BLT is the first branch control independent of BGE – meaning that it can be reached on all paths from BGE. The first instruction in the basic block belonging to BLT is called the *reconvergence point* of BGE. A conventional processor would squash, along with any other wrong-path instructions, the reconvergence point instruction and all subsequent instructions on misprediction of the protected branch. This is wasteful because these instructions are soon refetched after the squash. In the selected benchmarks used in this study, the number of cycles it takes a branch to resolve vary from 30 to 140, with the average being 40. Since there are 8 instructions fetched per cycle, this means that on average there are potentially 320 instructions that may be squashed upon a misprediction. Since many branches have reconvergence points nearby (usually less than 16 instructions [CTW04]) there is high potential benefit for CIPs.

There are several implementation issues of control independence that can ruin its potential for benefit. In the introductory example, the later squashed **taken path** block of code changed the value of register `r3` before the squash. The CIP must re-execute the post-reconvergent instructions with the correct value of `r3` (the value it was set to before the branch). This is just one

example of implementation issues that CIPs must address to maintain program correctness while fetching out of order. Realistic mechanisms implemented to maintain program correctness are required for any CIP implementation.

3.1 Implementation Issues

3.1.1 CD- or CI-First

There are two fetch techniques a CIP may implement. *CD-First* is a technique where a CIP fetches just as a conventional system would until a protected branch resolves. If it resolves correct, execution continues similarly to the conventional case. If it resolves mispredicted, only CD instructions are squashed. The correct path instructions will be fetched and executed while any post-reconvergent instructions are still in flight. Once the entire CD region is fetched, fetching continues at the point where it was at the moment just before the protected branch resolved. The post-reconvergent instructions may need to be re-executed in order to maintain program correctness. The example given in the introduction reflects this technique.

CIPs that employ the *CI-First* technique begin fetching post-reconvergent instructions immediately after fetching the protected branch. Once the branch resolves, the correct path CD region is fetched and executed. Similarly to the previous technique, after the CD instructions are fetched, the post-reconvergent instructions may need to be re-executed to maintain program correctness. Notice that this technique eliminates the need to initially predict a direction for protected branches and so there is no need to squash.

3.1.2 Register Remapping and Speculative Execution

Dynamically scheduled processors map an instruction's destination register to a freshly allocated physical register and read mappings for the instruction's source registers. This mapping enables

instructions that write the same architected register to execute out of order. Since they write different physical registers, no data is lost.

The mappings of instructions past the reconvergence point may depend on the path taken through the control dependent region (CDR). In execution, it is common to have register dependencies between the CDR and post-reconvergent instructions. The CIP may not be aware of these dependencies until a protected branch resolves. Once the correct CDR is fetched, the register mapping becomes defunct and must be repaired to maintain program correctness. Therefore, any CIP must take the steps needed to correct register mappings when performing a protected recovery.

Some CIP implementations correct the mapping using *injected instructions* [CV01, AZRRA07]. After executing the CD instructions and before continuing execution of post-reconvergent instructions, special MOV instructions will correct the mapping. The example at the beginning of this section refers to the register r3 of Figure 1.1. Assume the code in the figure is running on a CIP and that the “Taken Path” block was just squashed while the post-reconvergent code is still in flight. At this point, the MUL instruction has operated on the incorrect value of r3 . To repair this, the CIP will inject a special instruction into the pipeline that will write the value of r3 to the value that it was before the incorrect CDR changed it. This way, post-reconvergent instructions may re-execute using the correct value.

Instructions that depend on registers that may be incorrect must be executed speculatively until any downstream CD region resolves. Once the register mapping is correct, dependent instructions are re-executed. Furthermore, instructions that consume data from these instructions must also be re-executed, and so on. When a branch is re-executed, *vacillation* may occur. A branch vacillates

when it changes its resolved direction due to re-execution. It is possible for a single instance of a branch to vacillate more than once. Vacillation is a very important overhead of CIPs. Its impact to combat certain types of weakening will be elaborated further in the study.

3.1.3 Finding the Reconvergence Point

Reconvergence point detection is crucial in a CIP because it partitions the control dependent and control independent instructions for a protected branch. There are several techniques that find or predict it with reasonable accuracy both statically [SBV95] and dynamically [AZRRA07, CV01]. In one dynamic implementation [Kop08], each of the instructions on separate paths flowing from the protected branch are tagged with a different color for each path. The reconvergence point will be the first instruction tagged with both colors. Since the CD region is found dynamically in this way, the candidate branch must execute at least once on both paths. The mechanism also considers return instructions. If both paths from a protected branch lead to a return, the reconvergence point would then be the target of the return.

In a separate implementation [CV01], the reconvergence point can be found dynamically by searching for `if then else` and similar control flow structures. This is done by checking if the first instruction after a branch (not including delay slot instructions) is the target of a recent branch. Higher level constructs like `if then else` and `case` have easily identifiable reconvergence points. For example, the `if` clause and `else` clause are control dependent while anything after the `if then else` construct is control independent.

An advanced and highly accurate dynamic reconvergence prediction scheme was introduced in a study by Collins et al. [CTW04]. Branches are classified into several categories that are defined using analysis of program control flow graphs. For example, the most common case is

for a branch's reconvergence point to occur later in code (meaning the reconvergence point's PC is greater than the branch's PC), while no instruction past the reconvergence point ever executes in the CDR for some level of the function call stack. This case is handled by the reconvergence predictor that skipper utilizes; however, skipper assumes certain compiled instruction layouts and only handles this single case. Another case handled in the study, though not as common, occurs when there are multiple return instructions in the CDR. An aggressive hardware implementation that categorizes branches into one of four behaviors, including those just presented, predicts reconvergence points with 99.9% accuracy for most of the studied benchmarks. A more feasible implementation of the predictor achieves over 95% prediction accuracy.

3.1.4 Selective Squashing

In conventional systems, instructions are kept in the *re-order buffer* (or similar) from the time they are initially fetched until they are committed or squashed. The re-order buffer (ROB) is generally a FIFO that serves many critical functions. It assures that instructions commit in order (though they may execute out of order) and provides a means for recovery upon branch mispredictions or exceptions. Control independence exploitation poses a problem for conventional ROB's due to out-of-order fetching. The ROB may need to be redesigned to leave a gap for any later incoming CD instructions when a protected branch is fetched.

In many implementations, the size of the gap can be guessed similarly to the way reconvergence points are predicted. Accuracy in gap size detection is crucial since all instructions after the protected branch will have to be flushed if the gap size is inadequate. Furthermore, overshooting the gap uses unneeded space in the instruction window which may eventually cause the fetch unit to stall.

3.1.5 Targeting Branches That Are Difficult to Predict

A CIP implementation may turn protection for branches on (and in some cases, off) during execution [RSI, AZRRA07, HR07, CV01] while another may protect every instance of certain static branches [CFS99, SBV95]. In the former case, referred to as a *dynamic CIP*, some method like *confidence estimation* (described in the next paragraph) is used to dynamically determine candidates for branch protection. In the latter case, called a *static CIP*, some type of instruction set architecture support is necessary to convey information regarding candidates for protection to the system. This information may be generated by the compiler by way of techniques such as static code heuristics or training input sets.

Confidence estimation is a technique used to detect if a branch is likely to be mispredicted. A study by Erik Jacobsen et al. presents several different one- and two-level confidence estimators [JRS96]. In one of the more successful one-level implementations, a table called the *Correct/Incorrect Register Table*, or CIR Table, is indexed similarly to a PHT to yield whether or not a branch is likely to mispredict. Each entry of the CIR Table is 4-bits, and each of these entries are initialized to all ones. A branch is considered likely to be predicted correctly if its CIR Table entry is 15. If a branch is predicted correctly, this entry is incremented (though it saturates at 15). If the branch is mispredicted, the entry is reset to 0. This relatively simple technique proves effective, isolating nearly 90% of mispredictions for selected benchmarks.

For a detailed comparative analysis on the confidence estimation method described above as well as several other techniques, consult the study by Grunwald et al. [GKMP98].

3.1.6 Areas of Low Potential for Benefit

Not every application benefits from control independence. There will be little benefit in protecting branches with a very distant reconvergence point. The hindrance is due mainly to the amount of instructions that will be squashed on a protected recovery. A CIP may also not show much benefit if the CDR contains dependencies along the critical path. Though the post-reconvergent consumers will not be squashed, they will have to wait for the protected branch to resolve anyway. This generally increases the number of in-flight instructions and could cause the ROB to fill, stalling the fetch unit. Additionally, codes high in weakening and vacillation tend not to benefit and in some rare cases may exhibit performance degradation. Nevertheless, the majority of applications in the benchmark set selected for this study enjoy the benefits of control independence.

3.2 Snipper

Snipper is the CIP selected to be used for this study [Kop08]. It is named so because the term *snip* is used to refer to a control dependent region and its context. It attains speedup competitive with other researched CIPs, but does so in a unique way. As other CIPs choose where to exploit control independence based solely on branch confidence estimation [CV01, HR07] or detection of a reconvergence point [AZRRA07], snipper additionally uses a performance estimator to judge where exploiting control independence would be beneficial. This is helpful, as there are common situations where protecting branches may not result in speedup or may even hinder execution.

Protecting a branch is not beneficial when the branch is *execute-* or *commit-critical*. As defined in a study by Fields et al., a branch is execute-critical when there is a critical path data dependency in its CD region [FRB01]. Exploiting control independence in this case does not help since it is the branch's resolve time that is the bottleneck. In fact, mainly due to vacillation, covering

execute-critical branches can in some cases lengthen the resolve time of other branches, causing slowdown. A branch is commit-critical when it is the next instruction to commit and is preventing other instructions from being fetched because the ROB is full. In other words, the CPU cannot accommodate more instructions until the branch commits. If the system's instruction window size were larger, the branch would no longer be commit-critical.

Snipper protects branches only when its *reduction estimator* detects possibility for speedup. The reduction estimator used for this study, named *fetch-cycles*, evaluates whether or not a branch is execute- or commit-critical. It does so by way of bookkeeping certain characteristics of snips. For example, one of the values recorded is number of cycles spent fetching CI instructions from when a branch is mispredicted until it is resolved. The estimator also checks for a full ROB as well as whether or not the branch is near the head of the ROB. For more details on reduction estimators, a thorough study has been conducted by Koppelman [Kop08]. In the study it is shown that using such reduction estimators avoids slowdown in areas of execution where control independence cannot be effectively exploited.

At a lower level, snipper is a relatively simple CD-First CIP. Instructions are re-executed without changing their original register mapping. It does this by injecting special MOV [SI94] instructions called *pmoves* [KG99] that correct values in the mapped physical registers of control independent instructions. More than one pmove of any architectural register may have to be injected, depending on the number of times the register was written in the doomed CDR. Using the injected instructions allow post-reconvergent consumers to remain in the scheduler without having to be renamed, though they will need to re-execute.

Information for snips is kept in a *snip information table*. This table includes data such as the

candidate branch's PC, the reconvergence point, and a score used to determine whether or not exploiting CI for the candidate branch is detected as worthwhile. The reconvergence point is found using the coloring method described in Section 3.1.3. The colored tags are referred to as *cookies* in the sniper nomenclature. Information about cookie locations is kept in the *cookie table*.

Snipper turns protection of a branch on and off depending on whether or not potential benefit is detected. This is useful when the path to a protected branch changes at different points in the program; for instance, if the branch is in a subroutine called from many different parts of program execution. The reason for dynamic protection of this caliber is that, as has been said, sometimes exploiting control independence does not help. Snipper can also run as a static CIP so that each static branch is either always or never protected. More information regarding this is provided in Section 5.2.

The default predictor used by sniper is the YAGS predictor developed by Eden and Mudge [EM98]. This predictor correlates branches on global outcome history via the GHR. YAGS is not used in this study since the way in which it makes predictions is more complex than GShare. Nevertheless, the hybrid predictor used here performs just as well or better for most benchmarks and is more widely studied.

Snipper's approach to history update is to always insert CDR data into the GHR and use it for prediction and update, regardless of whether or not it is correct. This method is used because it yields better results than not including CDR data into the global history.

Figure 3.1 shows the speedup of a system exploiting control independence using sniper. Results are shown for the system branch predictor as bimodal, GShare, and hybrid.

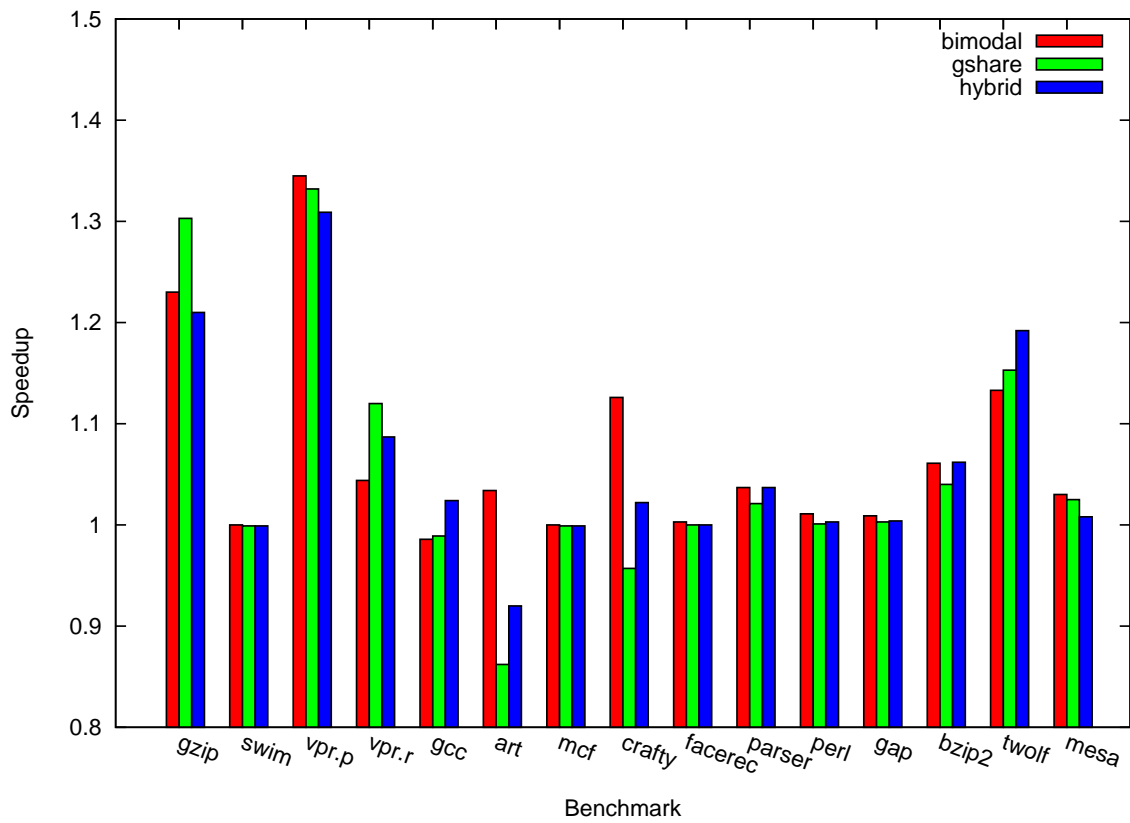


Figure 3.1: Snipper Speedup (petdis.69, pad-cdr)

Snipper is described here only to the point of detail necessary to discuss branch weakening.
For more details, consult the study by Koppelman [Kop08].

Chapter 4

Prior Work

4.1 Limit Studies

Several studies have qualified that returns of exploiting control independence are worthwhile. A study by Lam and Wilson shows the amount of parallelism that can be obtained with control independence exploitation on an abstract system [LW92]. The system models used in the study enforce true data dependencies and control flow while ignoring memory disambiguation, non-true data dependencies, and resource limitations. There are an unlimited number of functional units and instructions are fetched and committed in one cycle. The system model of interest for the purposes of control independence as studied here is the SP-CD-MF model. It is an ideal control independence system with multiple flows of control, meaning branches may execute out of order and only CD branches will be squashed on a misprediction. This model can be compared to another model in the study named SP. SP is simply a system modeled with only a branch predictor. Each system uses a perfect static predictor for branch prediction. Results show that the SP-CD-MF system can attain 23 times the parallelism of the SP system on average across the selected non-numeric benchmarks. When limiting control flow by forcing branches to execute in program order (this is the SP-CD model), the speedup over the SP system drops to about 15. The study concludes that parallelism is highly limited by control flow in certain programs and though branch prediction is vital in extracting reasonable amounts of parallelism from them, control independence significantly helps achieve large amounts of ILP.

Rotenberg et al. similarly compare a set of ideal machine models to evaluate several aspects of

control independence [RJS99]. The major difference from the Lam and Wilson study is that the models respect the need for register remapping and resources used by doomed CD instructions. As opposed to gathering results from a trace, a pipelined 16-way system with a GShare predictor is simulated. The model ignores the handling of memory disambiguation, output dependencies, and anti-dependencies. In addition to wasting fetch bandwidth, doomed CD instructions waste other resources by remaining in the instruction window until they are squashed. Data dependencies between doomed CDR instructions and post-reconvergent instructions are repaired in one cycle. It is reported that a model CIP with a 512-instruction window can cut down execution time 17% on average for the selected benchmark set.

4.2 Branch Classification and Prediction Techniques

Later in this study, weakened branches will be classified by the reason they are weakened. Additionally, predictor techniques will be offered to alleviate the preventable weakening by modifying paths and predictor update times. There has been a significant amount of prior works that identify ways in which path modification can improve prediction accuracy. Significantly less has been published in classification of branch mispredictions. The studies presented in this section contribute to the techniques used here to classify and reduce weakening.

An early study by Po-Yung Chang et al. classified branches by the rate at which each static branch is taken [yCHyYP94]. When branches are classified in this way, certain predictors can be chosen to predict certain classes of branches. For example, if a branch is classified to be mostly taken, a static predictor can often perform just as well or better than a correlating predictor in predicting the branch. The study introduced several hybrid schemes that performed as well or better than other branch predictors in literature at the time. In a more recent study by Michael

Haungs et al., branches are classified by the rate at which they change direction [HSF00]. These studies use branch classification to build better predictors. In this thesis, however, classification is used to gain an understanding of why certain mispredictions are caused. There are no efforts taken to extract performance directly from the classification.

In a study by Kevin Skadron et al., a broad range of predictors are used to develop a taxonomy of mispredictions [SMC00] to help understand why certain branches are mispredicted. The selected predictors for the taxonomy are chosen carefully based on the information used to make a prediction. A dynamic branch is predicted through a sequence of chosen predictors. The first predictor that correctly predicts the branch instance determines the reason for which previous predictors in the sequence mispredicted it. For example, in the sequence of tests a branch may be mispredicted by a correlating predictor. The next predictor in the sequence could be a bimodal predictor. If the bimodal predictor yields a correct prediction, then it can be assumed that the correlating predictor's misprediction is due to training a new path. In the study, a new predictor scheme named *alloyed prediction* is developed to fill a hole in the taxonomy by categorizing mispredictions due to unavailability of both local and global history. Such study of branch predictor behavior is of great importance to understanding the causes of weakening.

Paths may be manipulated via code transformations to allow for better prediction accuracy. In a study by Cliff Young and Michael D. Smith [YS99], a code generation technique used to obtain better prediction accuracy for correlated branches is explored. A *history tree* is built from a program's *path profile* that contains all paths leading to a particular branch. A path profile is a type of lightweight program trace. Through a technique called *pruning*, the history tree is transformed so that the minimum amount of history to exploit correlation is revealed. Code is

transformed using the pruned trees to allow bi- branches to be duplicated so that each copy of the branch is a mono- branch. The proposed code transforms could improve execution time by as much as 4% for selected SPEC CPU 1992 and 1995 benchmarks, though the technique slowed go and jpeg down by 1-2% due to additional instruction cache misses.

Paths may also be manipulated dynamically to reduce mispredictions. Multi-threaded execution has the potential to weaken branches because, like in CIPs, branch outcome history is not available in contiguous program order. In a study by Jayanth Gummaraju and Manoj Franklin, the effects of single-program (instructions commit in order) multi-threading on branch predictors are explored [GF00]. It is established in the study that multi-threaded processors' branch prediction accuracy is negatively impacted due to several reasons. The study names the reasons insufficient, discontinuous, outdated, scrambled, or inaccurate history. These different reasons can cause up to five times more mispredictions for a predictor like GShare on select SPEC CPU 1992 and 1995 benchmarks. It is shown that predictors that use global history are affected much more than predictors like PAg that use local history, mainly because local predictors are less prone to outdated information. An *extrapolation/correlation hybrid* predictor is developed to address outdated and scrambled histories. The predictor has two components. The first component uses in-order speculative outcome data to make predictions of branches. This is helpful since update lag is relatively high for single-program multi-threaded execution. The second component, the correlation-based predictor, chooses one of several extrapolation predictors based on a thread-level prediction. The predictor reduces mispredictions by around 3% for most benchmarks.

In another study on path manipulation for multi-threaded processors, Bumyong Choi et al. built upon Gummaraju and Franklin's study by focusing on branch prediction for branches in

short threads [CPT08]. Since small threads don't contain enough history for correlating predictors to function effectively, setting the GHR to a thread's initial PC upon spawning reduced the misprediction rate by around 29% per thread for a system with a GShare predictor running select SPEC 2000 benchmarks. This technique allows branches in short threads to correlate to the thread itself, allowing for less overall training. Leo Porter and Dean M. Tullsen generalized this technique for a conventional system [PT09]. In the study, it is found that setting the GHR to the value of the PC in certain situations – namely when leaving a loop – can reduce the misprediction rate by 12% per kilo-instruction for 32Kb predictors. A small 8Kb or 16Kb GShare predictor using this technique can perform as good as one twice its size.

4.3 Early Control Independence Processors

4.3.1 Multiscalar

The Multiscalar processor is a multiprocessor which exploits ILP by using a compiler to split a program into many tasks, each of which is dynamically assigned to one of many processing units [SBV95]. Each processing unit sequentially executes instructions within its task, and the tasks themselves are loosely sequentially executed. Register mappings are kept correct through the use of compiler inserted masks that forward producer registers between processing elements to future tasks. This serves the same function as the injected instructions mentioned earlier. A task predictor speculatively assigns tasks to processing units. On a task misprediction, the offending task and all following tasks are squashed. However, a mispredicted branch within a task whose control does not leave the task will only cause its own task to be squashed. Because of this, the compiler's job of constructing tasks becomes very important. Multiscalar processors exploit enough control independence to enjoy 2-3 speedup in many chosen benchmarks. Evaluating the

weakening caused by using a multiscalar approach is difficult since the multiscalar compiler-generated code is significantly different from code compiled for a conventional processor with respect to control transfer.

4.3.2 Dynamic Control Independence

In a study by Yuan Chou et al., a second ROB called the *Dynamic Control Independence*, or DCI, buffer is used to avoid refetching and renaming control independent instructions upon misprediction of a branch [CFS99]. The study explores both a CI First and CD-First implementation. It enables control independent instructions that have no CD data dependencies to be copied into the ROB from the DCI on protected recovery without needing re-execution, though branches are always re-executed. The implementation uses a GShare predictor that is stated to have “realistic” update, but no further information is given about how history is inserted into the GHR. The DCI study presents that in an 8-way superscalar processor with a 240-entry ROB can improve performance by about 15% among selected SPEC CPU 95 benchmarks [DR95]. Although in nearly every case the CI-First implementation outperforms the CD-First, the authors of the study claim that the latter appears to be more effective than the former since an unrealistic confidence estimator was used.

4.3.3 Skipper

The Skipper implementation by Cher and Vijaykumar is a CI-First CIP [CV01]. Skipper protects only low-confidence branches using a confidence estimator that dynamically tracks branch performance [JRS96]. Skipper finds the reconvergence point of a protected branch by examining common compiler constructs such as those derived from if-then-else statements. If needed, register mappings are corrected using injected instructions. Downstream instructions are then re-

executed appropriately. In order to avoid the unfavorable effect out-of-order fetch has on branch prediction, the hybrid predictor used by Skipper is set to update at commit. Misprediction rates between Skipper and a conventional system are given in the study as the ratio of incorrectly predicted and unsuccessfully skipped branches to the number of total branches. However, more information is needed to determine if unprotected branches are being weakened, such as conventional accuracies discounting branches that snipper would protect.

4.4 Transparent Control Independence

The Transparent Control Independence (TCI) study implements a CD-First CIP where speculative CD regions of protected branches have less demand on the system pipeline [AZRRA07]. If data dependencies are broken due to a protected branch misprediction, a special afore-generated “recovery program” is fetched into the pipeline to correct broken register maps. TCI implements the behavioral dynamic scheme to find reconvergence points developed by Collins et al. [CTW04]. Protection of branches is governed by whether or not a branch’s reconvergence point is detected. Post-reconvergent instructions that are data dependent on some speculative CD data are kept in a memory buffer near the pipeline. On resolved misprediction of a protected branch, the recovery program repairing register maps and the checkpointed data-dependent post-reconvergent instructions are injected into the pipeline for re-execution. If the protected branch resolves correct, instructions are removed from the buffer. TCI leaves outcomes from mispredicted CD regions out of the GHR.

The TCI architecture achieves speedup of around 1.2 on average for an 8-instruction wide fetch unit among 15 SPEC CPU benchmarks. Out of 15 benchmarks, 10 suffered weakening. Among these, weakening raises misprediction rates by 7.7% on average, the worst case raising

the misprediction rate by 24%. TCI utilizes a complex perceptron predictor [JL01] to achieve a reasonably high prediction accuracy and to produce results that aren't inflated. It is explicitly mentioned in the study that the weakening is caused by gaps in the global history, and that the perceptron predictor is more resilient to these gaps than GShare. There is no further look into weakening, as TCI is said to have been designed to tolerate some extra mispredictions.

4.5 Ginger

The CD-First CIP Ginger developed by Hilton and Roth [HR07] uses a method called “tag rewriting” to eliminate the need to inject instructions on a protected squash. Doing this aims to lower hardware demand when register maps need repairing. It uses a confidence estimator to dynamically protect branches [JRS96]. Reconvergence points are found statically and are inserted into the pipeline as “hints”, which are discarded at decode. After a protected squash, the pipeline is stalled so that register maps can be repaired.

Perhaps the most attention to weakening in all proposed mechanisms is given in the Ginger implementation study. In fact, it is mentioned explicitly that control independence interferes with conventional branch predictors due to weakening: “It would be counter-productive if Ginger induced more mispredictions than it tolerated.”[HR07] The implementation attempts to resolve weakening using two separate predictor states. One excludes any CD history outcomes from its global history. When using this, the prediction accuracy is preserved for branches not correlated to CD outcomes. To accommodate for cases where branches may be correlated to these outcomes, a second predictor state is added that uses contiguous global history. A chooser is used to extract the best prediction of the two states. It is said in the study that the table used in the latter predictor can be small because the number of branches that correlate to CD data is small. No further

evidence is given to support this claim other than overall performance results. It is shown that this scheme improves performance only slightly as opposed to using a predictor that does not contain CD information in its GHR. In some cases, performance may lower when using the dual scheme. One interesting result shows that using a scheme that excludes CD data from history can actually perform better than the perfect in-order case since there are more useful outcomes that would otherwise not appear in the global history.

Chapter 5

System Simulation Methodology

All results in this study were gathered and evaluated using simulation of a conventional system and a CIP system. Timing simulations are performed on near-future configurations of these systems. This chapter will cover the simulation software, branch predictors, system configuration, and benchmarks that have been chosen.

5.1 Simulation Software

All experiments are conducted on a heavily modified version of RSIM [HPRA02] named RSIML [RSI]. RSIM is a conventional CPU simulator developed at Rice University to research instruction level parallelism in shared-memory processors. RSIML is developed at Louisiana State University and adds several relevant features including control independence exploitation, GShare and hybrid branch predictors, as well as branch prediction at the block level [Kop02], speculative multithreading (enabling out-of-order fetch), functional simulation mode, and multiple branch prediction. The simulated processor implements the SPARC v9 [SI94] instruction set architecture sufficiently to support every instruction of the chosen benchmarks compiled for real systems. Additional modifications enable RSIML to run ordinary Solaris binaries (that is, there is no special compilation or link steps). There is also the ability to perform pipeline-level timing simulation at selected locations while using high-speed functional simulation between them. RSIML runs on both Solaris/SPARC and Linux (x86 or x64) systems. All simulated benchmarks pass verification against SPEC-provided outputs. RSIML simulates to roughly the register-transfer level. Aspects of the system most relevant to this study are the sequencing of operations related

to branch prediction, including prediction and update times. RSIML realistically implements this sequencing.

All simulations were performed on several commodity clusters available through either the Department of Electrical and Computer Engineering or High Performance Computing at Louisiana State University. These clusters all run 64-bit GNU/Linux variants as operating systems. Simulation times vary depending on the amount of resources and number of simulated configurations. On average, a batch of simulations will utilize 64 processors and a wall time of about 12 hours. It has taken over 15,000 CPU-hours of simulation to generate useful results for analysis in this research.

5.2 Configuration of Simulated System

The base configuration of the simulated system shown in Table 5.1 is tuned to match similar CIP configurations Ginger and TCI. The 20-cycle decode-to-execute delay sets a lower bound on the penalty for a branch misprediction. Three additional cycles are needed for recovery timing, plus whatever time by which a branch resolution is delayed.

Configuration parameters for all base predictors used in this study are shown; the system uses only one of these at a time. Note that the bimodal/GShare predictor takes twice as much space as the GShare or bimodal predictors. There was no attempt made to equalize the cost of the predictors mainly because it complicates analysis: More coherent analyses can be made when using a consistent GHR length between the GShare predictor and the GShare component of the hybrid predictor.

Snipper can be very reactive to slight changes in its configuration. Some experiments in this study compare several similar predictor configurations to evaluate and fine-tune parameters of

Table 5.1: Configuration Parameters

Core		8-way superscalar 512-entry ROB 20-cycle delay from decode to execute 3-cycle delay for necessary recovery timing 8 integer ALUs, 4 floating-point ALUs Unlimited load/store queueing
Memory	L1 Instruction Cache L1 Data Cache L2 Data Cache Main Memory	64kiB, 8-way, 4 ports, 64B line size, 1 cycle latency 64kiB, 4-way, 64B line size, 1 cycle latency 8MiB, 8-way, 64B line size, 16 cycle minimum latency 150-cycle minimum access latency
Fetch Unit	GHR BHT/PHT Entry Bimodal/GShare Hybrid GShare Bimodal Indirect Jump Return Address	16 bits 2-bit saturating counter 64ki-entry choice table 64ki-entry GShare PHT 64ki-entry Bimodal BHT 64ki-entry PHT 64ki-entry BHT 64ki-entry GHR-indexed return address table unlimited return-address stack
Snipper		4ki entry snip information table 4ki entry cookie table Maximum 200 instruction evaluation Maximum 200 CDRs

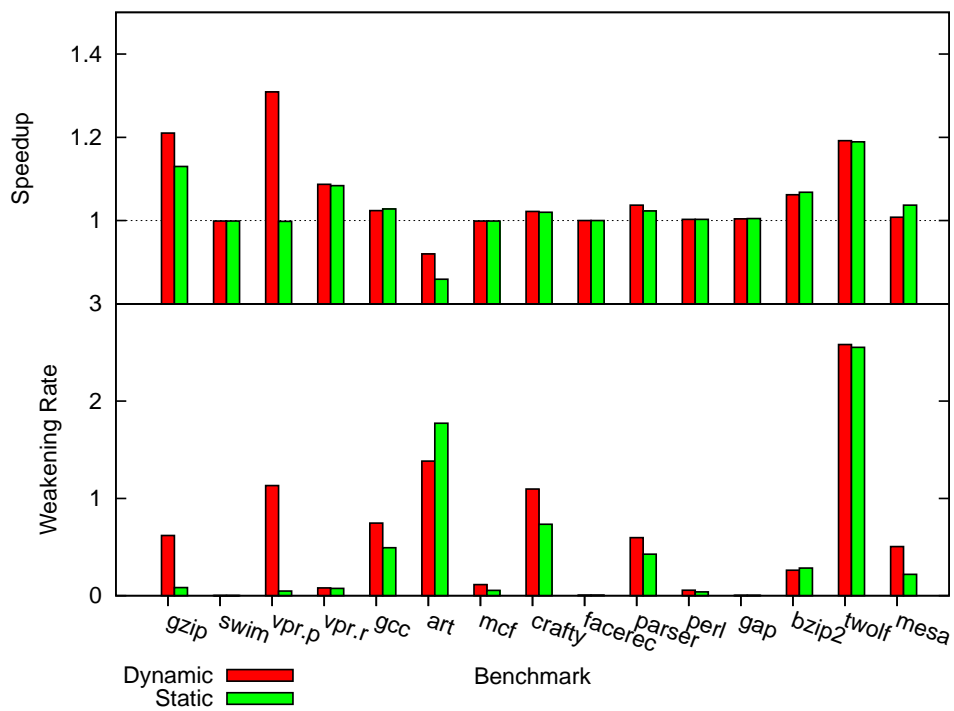


Figure 5.1: Static Snippet vs. Dynamic Snippet, Speedup and Weakening (petdis.111)

the predictors. Snipper running normally will dynamically turn protection on and off based upon a number of factors including branch prediction accuracies. This can interfere with attempts to cleanly measure weakening. Because of this, most results are gathered when snipper is running as a static CIP in which branch protection decisions were made before a run started using profile data. This way, a branch is either always protected or never protected in execution.

Snipper running as a static CIP is called *static snipper*. It determines which static branches to protect from profile data written in a previous training run. For this study, static snipper is trained using full reference inputs. Branches are protected in static snipper if their last dynamic instance was protected in the training run. Though training in this way is not practical, it allows for better analysis for weakening. For static snipper, most benchmarks exhibit similar amounts of weakening as the dynamic CIP version of snipper, called *dynamic snipper*. Figure 5.2 shows how dynamic and static snipper compare when using a hybrid branch predictor. Performance differences in training snipper with input other than the full reference input are not covered here. Unless otherwise noted, all remaining results use static snipper.

5.3 Selected Branch Predictors

The predictors mainly used in this study are bimodal, GShare, and bimodal/GShare hybrid. Diagrams of predictors are shown in Figure 5.2.

Though the functionality of each of these predictors has been described previously, there are some implementation issues that need highlighting. In the simulated system, the PC used to address the predictor table is the PC of first instruction in the corresponding branch's basic block (recall that the branch is always the last instruction of the basic block). In a conventional system simulation, the GHR will reflect the 16 most recent program-correct branch outcomes in program

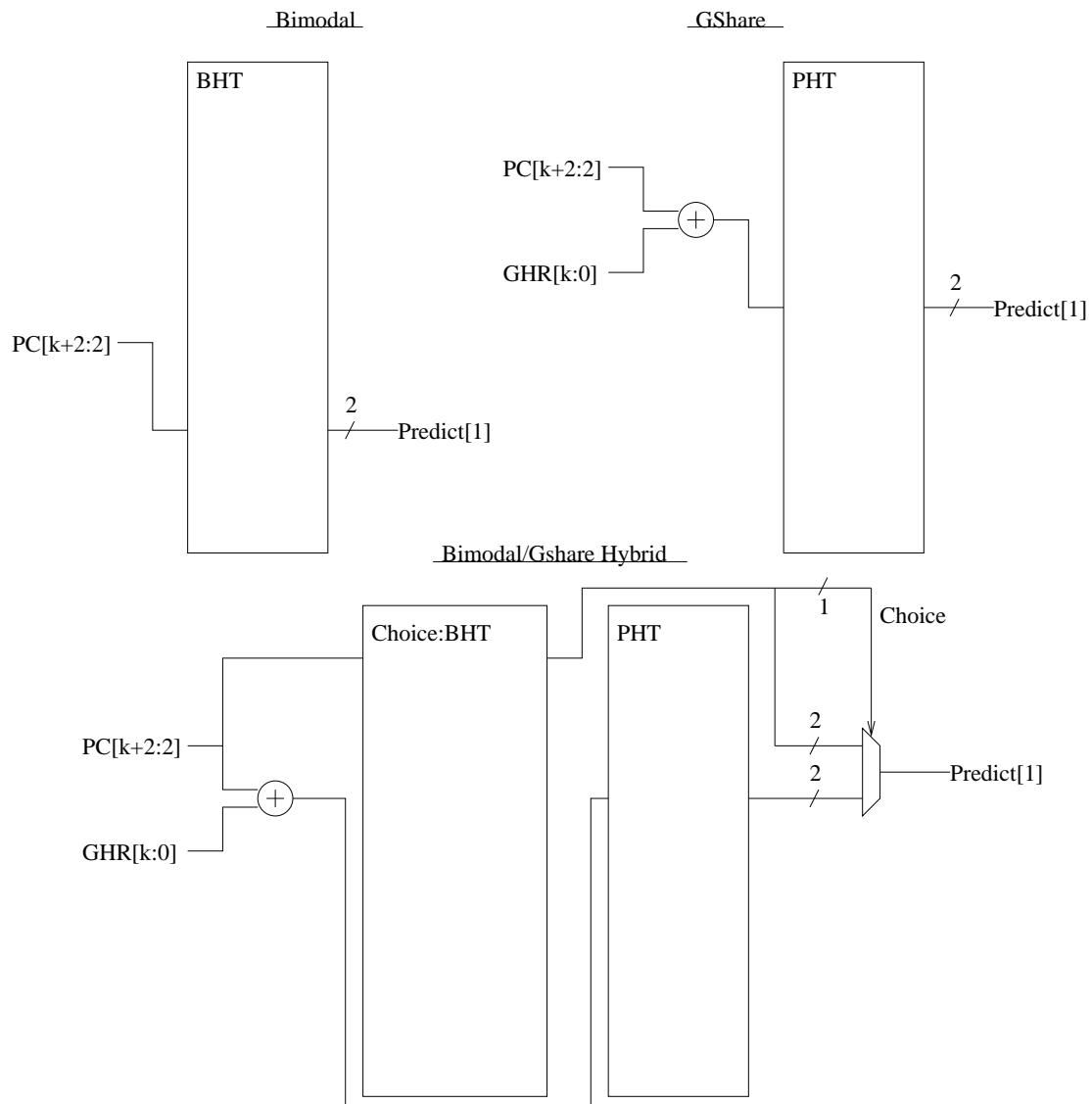


Figure 5.2: Branch Predictors Used in this Study

order. In order to maintain this correctness, the GHR is checkpointed and will be corrected for branch mispredictions. Exceptions and interrupting events can cause GHR corruption, but these occur infrequently, around once every 1 million instructions decoded.

The way in which a prediction is made is as follows. Assume a bimodal predictor of size 2^k . The BHT is indexed by the PC shifted right two bits. This is done because in the SPARC ISA, each instruction takes 4 memory locations. The least significant k remaining bits of the PC are then used to address the BHT entry from which the prediction is taken. GShare's PHT is indexed by taking these same PC bits and XORing them with the k -bit GHR. The hybrid predictor performs two table lookups in unison. The Choice:BHT is a per-address table similar to the bimodal BHT with the addition of a 2-bit chooser entry at each entry. The most significant bit of this chooser is used to select between either a bimodal or GShare prediction. Unless otherwise noted, all predictors are assumed to update at commit time. The GHR value used for the update is the one collected at predict time of the branch.

5.4 Benchmarks

The programs taken from the SPEC CPU 2000 suite [Hen00] to gather results are shown in Table 5.2. The suite contains both integer and floating-point benchmarks. There are 12 integer benchmarks, of which 10 are used in this study, and 15 floating-point benchmarks, of which 4 are used. The majority of benchmarks selected are among the ones that react, positively or negatively, to snipper activation and don't attain near-perfect branch prediction accuracy in the conventional system. There are a couple of arbitrarily selected benchmarks, namely swim and facerec. The benchmarks are compiled at high optimization levels with the Sun compiler [MS90]. Some of the longer benchmarks use the SimPoint targeted sampling technique [SPHC02] for reduction of

Table 5.2: Selected Benchmarks						
Name	Input	Static kI	Dynamic GI	misp/kI (bimodal)	misp/kI (GShare)	misp/kI (Hybrid)
art	input.graphic	61	164	2.9307	1.3703	1.2747
bzip2		76	0.196	8.3277	7.4838	6.9572
crafty		102	0.350	10.5107	5.1137	4.3724
facerec		235	285	6.2245	1.2003	1.2121
gap		190	206	3.1259	1.0136	1.0263
gcc		390	101	8.5937	4.9161	3.9916
gzip		86	98.5	12.3645	10.0950	9.8617
mcf		52	52.6	12.3015	8.5603	8.3706
mesa		230	162	7.6121	2.2430	2.1242
parser		124	347	20.2864	10.4086	8.9567
perlbmk	splitmail.850	214	104	2.3201	1.6581	1.5212
swim			210	0.0319	0.0264	0.0255
twolf		136	0.784	11.7819	8.9299	8.3291
vpr	place	143	0.182	13.0879	10.1551	9.6254
vpr	route	93	92.1	14.0338	11.3032	10.3836

simulation time.

5.5 Viewable Experimental Data

Discoveries and analyses of weakening were derived through examination of pipeline execution using PSE, a CPU pipeline visualization tool [PSEa]. PSE, short for Processor Simulation Elucidator and pronounced *see*, reads a data file generated by RSIML on each simulation. The file contains a complete record of the simulation run, including simulation host details, simulated configuration, and of course results of the simulation including data which allows visualization of instructions executed in the benchmark at the pipeline-level. For more detailed information on PSE, consult the cited homepage.

All results and examples presented in this study have an RSIML simulation batch name such as *petdis.111* provided somewhere in the figure caption or text. All output data from which analysis is done can be found at the repository used for this study [PSEb]. Each simulation

batch contains a vast amount of results such as decode slot usage and branch prediction accuracy presented as graphs and tables. More importantly, there is a link to the PSE data set of each simulated benchmark in the batch. This information is mainly supplied for ease-of-access and further study, but anyone may analyze the simulated data at their own discretion.

Chapter 6

Branch Weakening

Weakening causes misprediction rates to increase by up to 30%, robbing CIPs of significant performance potential. Before this study, there has never been any insight into how much weakening is avoidable or how much is an inevitable consequence of exploiting control independence. Moreover, the several causes of weakening have not yet been presented.

Figure 6.1 shows the weakening for dynamic sniper when using bimodal, GShare, and hybrid predictors. On average, misprediction rates rose by 22% across all predictors and selected benchmarks. Though many weakened benchmarks enjoy significant speedup when using sniper, there are several that suffer from weakening and do not benefit significantly from sniper. But how much of this weakening can be easily avoided and how much is impossible to avoid? Recall from the introduction that there are two broad reasons for weakening: changes in predictor update times, and changes to branch outcome history.

6.1 The Broad Classes of Weakening

The *absolute branch weakening*, or just *weakening*, from system X to system Y is defined as the number of mispredictions in system Y minus the number of mispredictions in system X . It is denoted $W^{X,Y}$. This definition is broad, but for the purposes of this study system X is fixed as a conventional system and Y is fixed as a CIP otherwise similar in configuration to X . Denote the total number of mispredictions on system X and system Y to be M^X and M^Y respectively. Then, $W^{X,Y} = M^Y - M^X$. Let B be some static branch. Define the number of mispredictions of B on X as $M^X(B)$ and likewise for Y , $M^Y(B)$. Branch B is said to be

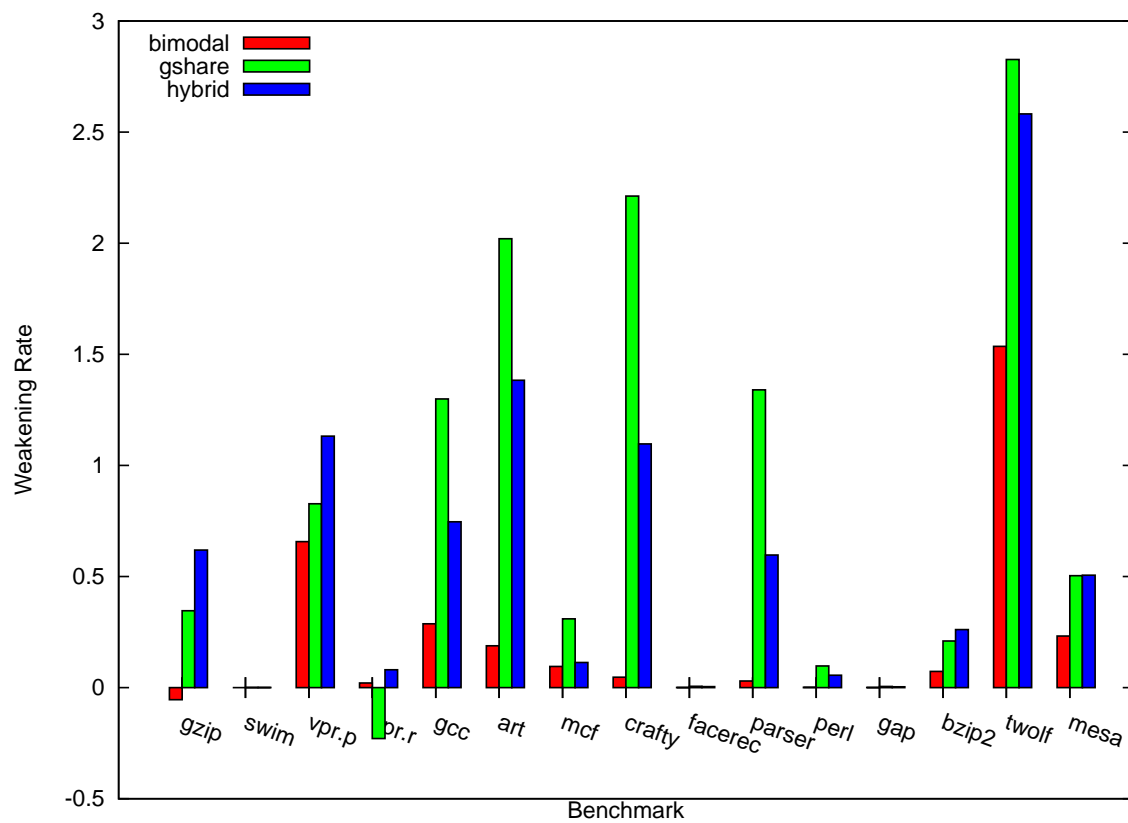


Figure 6.1: Snipper Weakening (petdis.111)

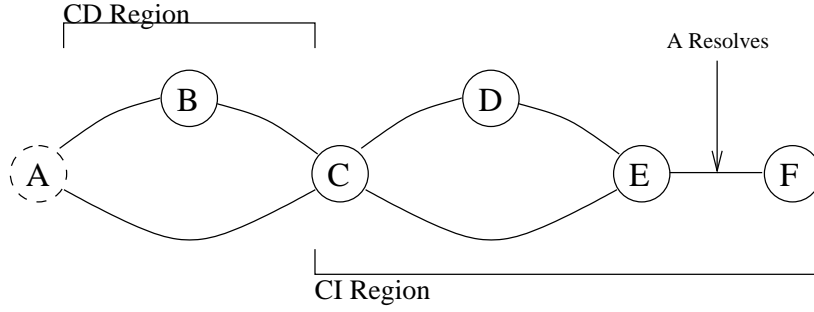


Figure 6.2: Example Control Flow of Execution

weakened if $M^X(B) < M^Y(B)$ and the *weakening amount* of branch B from X to Y , denoted $W^{X,Y}(B)$, is defined as $M^Y(B) - M^X(B)$. The *weakening ratio* is the weakening amount divided by the total number of successful protected recoveries in the CIP system. Only protected recoveries of those protected branches that commit are counted. Denote the misprediction rate on system X and system Y to be R^X and R^Y respectively. Define the *weakening impact* as $R^Y - R^X$.

Weakening occurs between CIPs and their conventional counterparts that use the same predictor. So, the weakening must be due to differences in prediction times and update times as well as differences in the outcome history used to make a branch prediction. Any weakening caused by differences in update and prediction sequencing will be referred to as *mangled-update weakening*. The correlating predictors in this study use a branch's path to index the PHT. Recall that the index is created by hashing the PC of the branch to the GHR. The GHR value in a CI system differs from that used in a conventional system. Any weakening due to this difference will be called *mangled-path weakening*.

These broad classes of weakening will be divided into subclasses and some will be studied in depth. For some subclasses, weakening can be reduced. For others, it cannot.

Each particular type of weakening will now be explained. Figure 6.2 shows a sample of exe-

cution control flow with each node representing a basic block ending with a branch. If there is only one edge exiting (connecting to the right side of) the node, the branch is biased. Assume the system predictor correlates on recent branch outcomes. The branch of basic block A, called Branch A or just A, is difficult to predict and so is protected. Assume all other branches shown in the figure are predicted with nearly 100% accuracy in the conventional system. The CI and CD regions are marked in the figure. The first instruction in the basic block containing Branch C is the reconvergence point of A. Notice that the protected branch A resolves far into the region of control independence. Define the *control path* as the sequence of basic blocks whose outcome histories will be in the path of a particular branch. Assume branch C is very highly correlated to A so that the two common control paths in the figure are ABCDE and ACE for the branch F.

The branch E – which is only observed on two control paths in a conventional system – could be observed on an additional two control paths in the CIP, ABCE and ACDE. This is because E is fetched before A is resolved mispredicted but is not flushed. These two added control paths require predictor training and the additional mispredictions are considered mangled-path weakening. This type of weakening can be lessened by using special history update techniques that prevent the speculated CIP paths from being observed in the system state. This specific type of weakening that causes the number of paths to increase is called *insulated weakening* because it increases the training time of the predictor.

Another type of mangled path weakening called *absentee weakening* is caused by correlation data not being available at a post-reconvergent branch's predict time. Referring back to the figure, say Branch D is highly correlated to B and is not correlated to any other branch. In a conventional system, the outcome of B is always available at D's predict time. Now consider a CIP where D is

Table 6.1: Branch Weakening Types		
Class	Subclass	Cause
Mangled Update	Delayed Update	Update lag
	Incorrect Update	Branch vacillation
	Shuffled Update	Out-of-order predictor update
Mangled Path	Soft Absentee	Loss of correlation data at GHR fringe
	Hard Absentee	Loss of correlation data from the CDR
	External Insulated	Noise ingestion at the GHR fringe
	Internal Insulated	Noise ingestion at the padded region

seen on the new path ACDE. The history data for B is not available when D is predicted. Therefore, D has nothing useful to correlate with, which causes absentee weakening. It is difficult to avoid absentee weakening when the outcome data needed lies in the CDR, so it may be favorable to disable protection of the branch causing it.

A milder form of absentee weakening occurs when important outcomes are pushed out of the fringe of the GHR. It will be shown that this weakening can be remedied using special outcome history update techniques.

When employing any CI technique, there may be longer predictor update times due to instructions' speculative execution when waiting for a protected branch to resolve. This causes an increase in predictor update lag. Weakening due to this is called *delayed-update weakening*. This type of weakening may be avoided by updating predictor tables earlier than commit time; for example, the first time a branch resolves. However, this early resolve can cause additional mispredictions when a branch updates the predictor with an incorrect outcome (before the protected recovery of some upstream branch).

Table 6.1 summarizes all the different types of weakening. The terminology in the table will be defined more precisely and discussed at length later in this chapter.

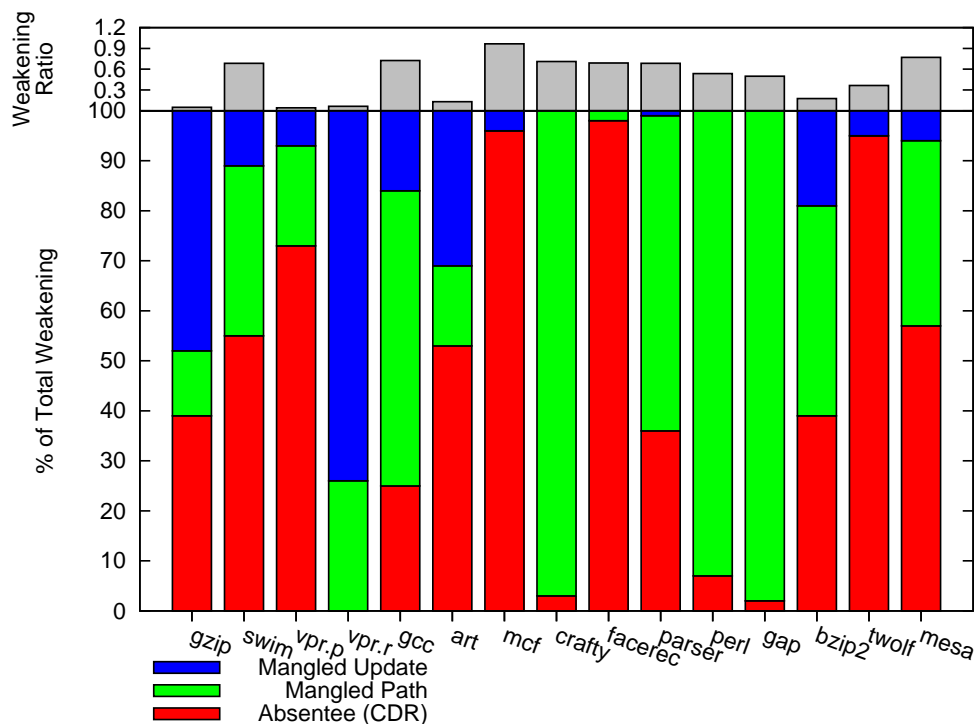


Figure 6.3: Weakening Classified by Type for Snipper (petdis.109)

6.2 Prevalence of Weakening Types

Figure 6.3 shows an approximation of the percentages of different types of weakening for the benchmarks. These results were collected using a snipper system with the hybrid branch predictor. In order to simplify results, the predictor in the snipper system is configured to not include CDR history in the GHR. Later, in Section 7, the method used to gather these classification results will be described in detail. The gray bar on the top part of the graph shows the respective benchmark’s weakening ratio.

The results show that there is no common pattern in the causes of weakening among the chosen benchmarks. Some benchmarks are predominantly affected by one type of weakening. Take gap as an example, where path mangling is responsible for all of the weakening in the program. The

crafty benchmark shows similar behavior. The majority of weakening for the twolf benchmark is absentee weakening due to unavailable CDR outcomes. Other highly weakened benchmarks like gcc, art, and mesa show more of an even mix of the three weakening types. Across all benchmarks, the most common cause of the three is absentee which is responsible for 45% of all weakening on average. Mangled-path weakening not including absentee weakening caused by unavailable CDR outcomes is a close second, causing 40% of the weakening. Though delayed-update weakening is not as prevalent, it is still far from negligible as many highly weakened benchmarks suffer from it.

6.3 Mangled-Update Weakening

6.3.1 Description

For reasons discussed earlier, CIPs have longer predict-to-commit times than conventional systems. Snipper induces nearly 5 cycles of additional update lag on average across all the benchmarks. This update lag could burden overlapping bistable branches and paths by causing an additional two mispredictions for every run.

There are several different types of mangled-update weakening. Recall that delayed-update weakening is due to update lag that causes branches to update predictor tables later than a conventional system. Based on analysis of the simulated benchmarks, this is the most prevalent type of mangled-update weakening for systems that perform predictor update at commit time.

Updating predictors before commit time has repercussions. Any branch outcome taken before commit time may be incorrect. Furthermore, updates can occur out of order. In a conventional system or a CIP, wrong-path instructions may incorrectly update predictor tables. CIPs addi-

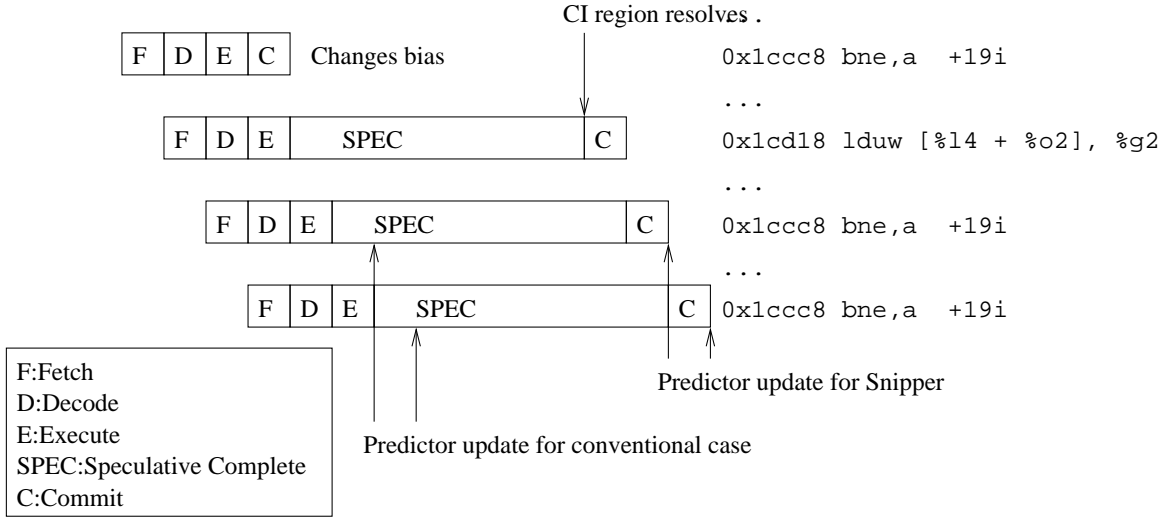


Figure 6.4: Example of Delayed Update Weakening

tionally have the burden of significantly more¹ vacillating branches which may cause incorrect updates. Weakening due to the additional out-of-order updates in a CIP is referred to as *shuffled-update weakening* and weakening due to the additional incorrect updates in a CIP is referred to as *incorrect-update weakening*. In this study, only delayed-update weakening is formally defined and studied in detail, but not without awareness of these other subclasses of mangled-update weakening.

Delayed update weakening may be reduced by updating predictor tables earlier than commit; for example, the first time a branch resolves. However, this does not always alleviate the damage because it may induce shuffled or incorrect update weakening. The goal of this section is to further explore the properties of mangled-update weakening. Through study of the update behavior of branches, mechanisms are developed to reduce this category of weakening.

6.3.2 Example

When presenting these real-life examples, the address of branches in hexadecimal is used. If there is interest, one can analyze the example themselves using PSE and the dataset [PSEb].

In the bzip2 benchmark, the branch at address `0x1ccc8` greatly contributes to overall weakening when using a bimodal predictor updating at commit time. The total mispredictions of the branch more than doubles when using Snipper. A closer look reveals that the branch exhibits a bistable behavior for most of execution. Figure 6.4 provides a simplified look at the pipeline execution of the loop containing the branch. The first shown instance of the branch is the final taken one, the following instances will all be not-taken. Note that the branch itself is protected, so subsequent instances are not squashed when it is mispredicted. Before the segment of code shown in the figure, there is a CD region that must resolve before the instruction at address `0x1cd18` commits due to dependencies. Because of this, the instruction must wait much longer than it would in a conventional system. Note the marked predictor update times for the different systems. The benchmark’s execution shows that the branch can be mispredicted as much as 6 times for each run.

6.3.3 The Effect of Delayed Update on Branch Prediction Accuracy

To gauge the impact of delayed-update weakening, systems with varying update lag were simulated. The graphs of Figure 6.5 show the impact of instruction update lag on branch prediction accuracy. The results were collected using functional simulations of the entire benchmarks. Predictor entries were updated a set number of instructions after their corresponding branches execute. The three results for each benchmark in each graph show the increase in misprediction

¹Vacillation can occur in conventional systems to recover from load/store dependence mis-speculation.

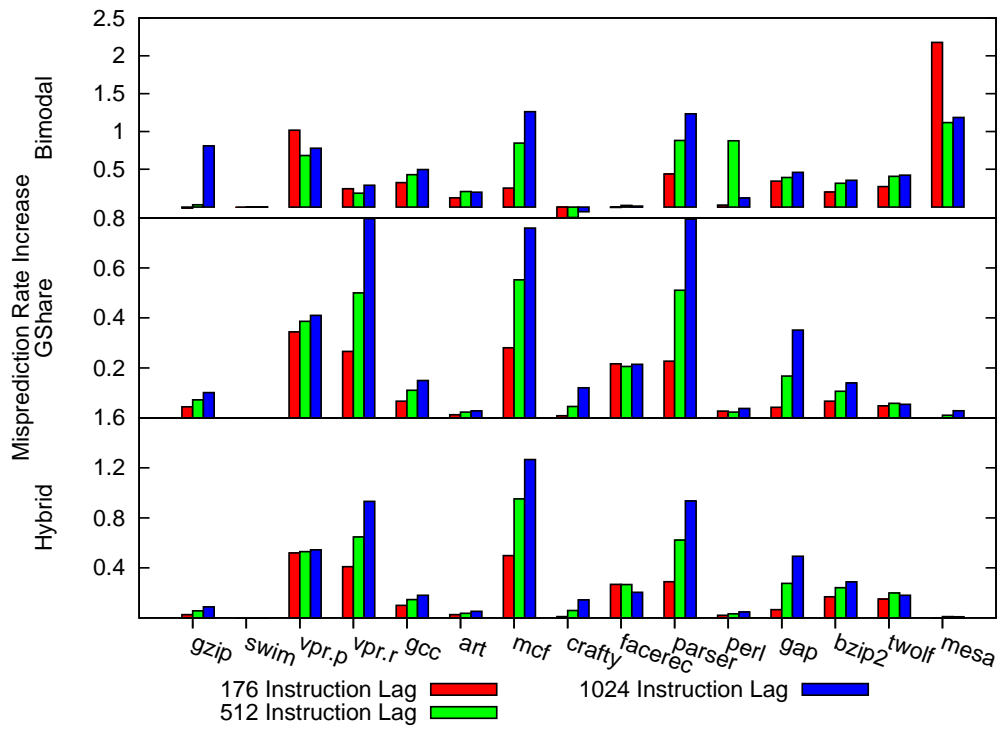


Figure 6.5: The Impact of Update Lag (petdis.115, functional simulation)

rate from a system with 0 instruction update lag to 176, 512, or 1024 instruction update lag.

For the system used in this study, at most 176 instructions may be fetched from the time a branch is predicted to the earliest possible time it can resolve. Therefore, the minimum instruction update lag when utilizing the full instruction issue width is 176. This is shown as the first result of each graph. The next result shows the impact of the maximum possible instruction update lag for the simulated system. This could happen if the re-order buffer was always full for the entirety of execution. The final result, an instruction lag of 1024, is included to show impact on systems with a larger instruction window.

It is evident that delaying the update of the predictor has noticeable impact on branch prediction accuracy. Trends in the majority of the benchmarks show that update lag in the 0-176 range has more impact than the 176-512 range. Still, the impact in both cases is quite significant for most benchmarks. Clearly, some benchmarks are much more affected than others. The hybrid and bimodal predictors are affected more than GShare. This follows the implications of branch and path overlap which were discussed in Section 2.4.

Increasing the instruction update lag from 0 to 512 increases the misprediction rate by 0.713 when using the bimodal predictor, 0.292 when using the GShare predictor, and 0.44 when using the hybrid predictor on average for the benchmarks. This is a good estimate ²of the maximum average impact of delayed-update weakening for the system configured for this study.

Because they are not squashed, control independent instructions in a CIP remain in flight much longer than in a conventional system. The time it takes for a protected branch to resolve roughly contributes to how out-of-date post-reconvergent predictions are. Covered branches that share

²It is an estimate because branches with erratic and hard-to-predict behavior can cause weakening to surpass the upper bound. The twolf benchmark, which contains many correlating branches very difficult to predict with a non-correlating predictor, exhibits this behavior for a bimodal predictor.

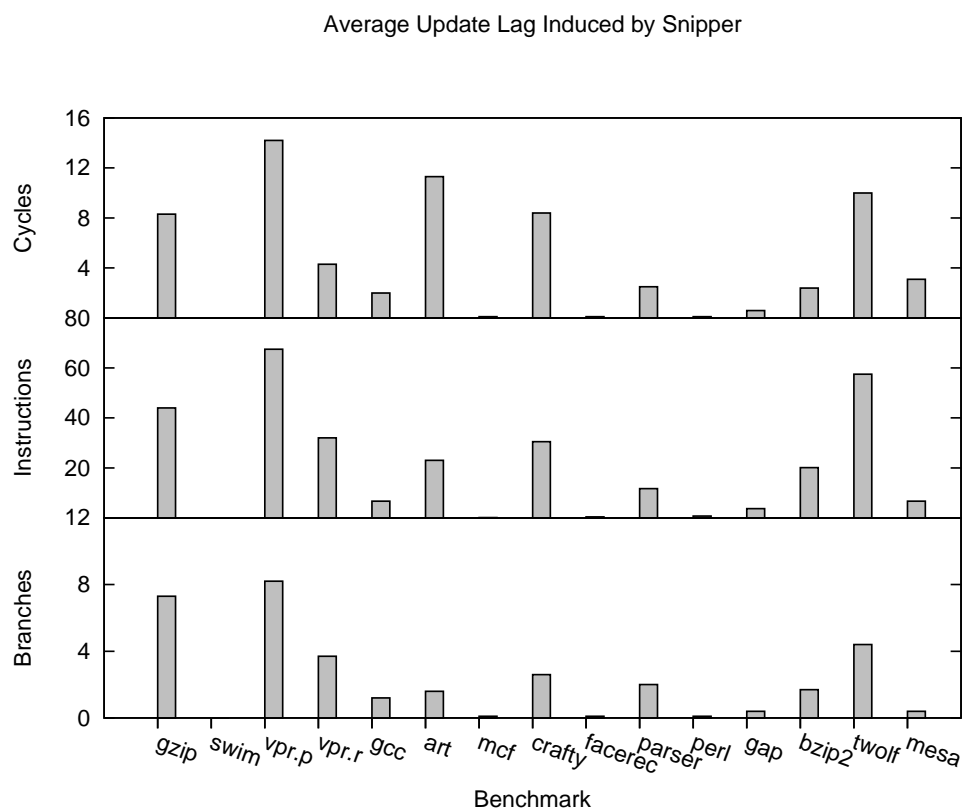


Figure 6.6: Update Lag Induced by Snipper (petdis.111)

data dependencies with CD regions before them must wait for earlier protected branches to commit. This can dramatically increase the update lag of any post-reconvergent branch. Predictions that are out of date typically hurt bi- branches because they require a quick update, as was exemplified with the example of Figure 6.4.

There is some delayed-update weakening in a CIP that is not so much involved with the increase of update lag, but instead with the fact that a protected branch's post-reconvergent successors are not squashed upon a misprediction. Non-doomed instances of these branches will be predicted much sooner than in a conventional system. For these instructions, the predictor appears to be updated much later in the CIP; hence, it is referred to as *update lateness*. Though update lateness is not directly caused by the update lag induced by sniper, it may be exacerbated by it. This type of weakening may be difficult to reduce since it requires predictor update before a branch resolves. Since it is directly related to update lag, this type of weakening is still considered delayed-update weakening in this study.

Figure 6.6 shows the average cycle, instruction, and branch update lag induced by sniper activation (the update lag in sniper minus the update lag in the conventional system). Notice that the benchmarks that exhibit more update lag are among the ones which significantly benefit from sniper. In the worst case, the branch update lag is 8. In situations where there are overlapping control independent bistable branches, this causes 8 additional mispredictions for every run. This effect could force an otherwise predictable branch to degrade in prediction accuracy to the point where it is marked for protection.

It has been established that update lag can significantly degrade branch prediction accuracy in most benchmarks. Sniper can induce an instruction update lag of 60. Though this is only a

Branch:	RT	RN	RN	RN	RT	C
Resolve:	UT	UN	UN	UN	UT	
Commit:						UT
First:	UT					
Change:	UT	UN			UT	
Change,Commit:	UT	UN			UT	UT

RT: Resolve Taken
 RN: Resolve Not Taken
 UT: Update Taken
 UN: Update Not Taken
 C: Commit

Figure 6.7: The Behavior of Predictor Update Schemes for a Vacillating Branch

fraction of the instruction window size, it is still enough to significantly reduce branch prediction accuracy for the majority of the benchmarks. This is especially true for the bimodal and hybrid predictors.

6.3.4 Reducing Mangled-Update Weakening

Protected recoveries start a wave of re-executing instructions, including branches. If a re-executed branch resolves differently than its previous resolution, it is said to vacillate. Setting predictors to update at resolve time rather than commit time can reduce delayed-update weakening for some branches but risks causing new mispredictions for others because vacillating branches may update predictor tables incorrectly.

There are many possible opportunities to update the predictor earlier than commit time for a dynamic branch instance. Branches may be updated every time they resolve, as shown labeled *resolve* in Figure 6.7. This technique is useful if the multiple resolves of a vacillating branch tend toward the branch's correct bias. A second technique labeled *first* in the figure only updates predictor entries at the first resolve of a branch. This technique is beneficial if having an early first guess that may be incorrect is better than having multiple updates. A more balanced method, *change*, only updates the dynamic instance's predictor entry on first resolve and additionally when a resolved outcome differs from its preceding resolved outcome. This method is useful

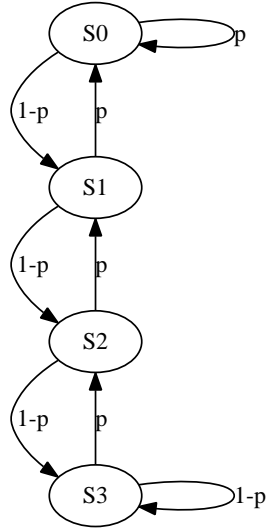


Figure 6.8: Markov Model of Predictor Entry State

when preventing drastic changes to the predictor entry is favorable. There are even still more update methods that may be used. As an example, a combination of the change and commit update methods is shown as the last example in the figure.

There is no update method of the ones described above that works best on all the benchmarks. The change, change-commit, and commit techniques yield the highest branch prediction ratios on average across all the predictors. Change performs the best on average, but a few benchmarks do not perform as well when using it. Among the studied benchmarks, there is no common favorite.

Vacillation is not very damaging when a single instance of a branch incorrectly updates the predictor, mainly because among most update methods an incorrect update of a vacillating branch will soon be followed by a correct one when the branch resolves correctly. However, with multiple dynamic instances of the same dynamic branch overlapping in execution, accuracy is likely to suffer. To better understand this characteristic, a model is developed and used to realize the effects of vacillation on branch prediction accuracy. The Markov chain shown in Figure 6.8 models the predictor state for a biased branch. States S_0 and S_1 reflect the two saturating counter states

that yield a correct prediction. For example, if a branch is biased taken and the predictor entry values 2 and 3 cause a branch to be predicted as taken, S_0 reflects the entry value 3 and S_1 reflects the entry value 2. If the branch is a branch biased not-taken, value S_0 then reflects the value 0 and S_1 reflects 1. The states S_2 and S_3 reflect the predictor entry not in the direction of the branch's bias.

The model assumes that many dynamic instances of the branch may overlap in execution. For example, one overlapping instance of a branch can set the predictor's state so that a subsequent overlapping instance of the branch is mispredicted. This is important since in a non-overlap case these branches would be predicted correctly.

Let n_r be the number of times in which a branch resolves per dynamic instance. The probability p that the branch's resolution will update the predictor entry correctly is then

$$p = \frac{\lceil \frac{n_r}{2} \rceil}{n_r} \quad (6.1)$$

when using the **change** update method.

The resolution of a single branch will follow a ...-wrong-correct-wrong-correct pattern. Consider a situation where there are many overlapping instances and where the predictor sees updates from these branches in an arbitrary pattern. We can then assume that updates are independent and so use the Markov model. The state probabilities for this model are

$$P[S_0] = \frac{p^3}{2p^2 - 2p + 1} \quad (6.2)$$

$$P[S_1] = \frac{p^2(1 - p)}{2p^2 - 2p + 1} \quad (6.3)$$

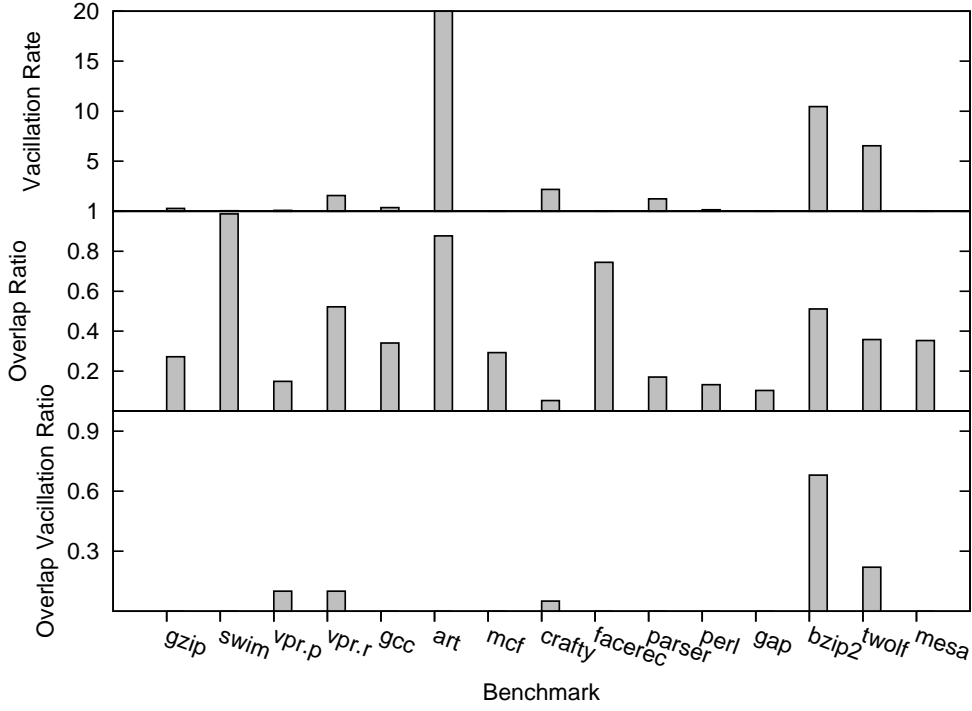


Figure 6.9: Overlap and Vacillation for Snipper (petdis.117, hybrid)

$$P[S_2] = \frac{p(1-p)^2}{2p^2 - 2p + 1} \quad (6.4)$$

$$P[S_3] = \frac{(1-p)^3}{2p^2 - 2p + 1} \quad (6.5)$$

This model assumes that predictions of the branch are made at random times. The probability of the predictor state being observed while it is incorrect is $P[S_2] + P[S_3]$.

The model highlights that if an overlapping biased branch always vacillates in a Snipper system, its probability of being in a correct state goes from 1 to 0.5. If the branch always vacillates twice, its probability of being in a correct state is slightly more (0.53).

The amount of vacillation and overlap for snipper using the change update method and a hybrid predictor will now be presented. Define the *vacillation rate* to be the amount of branch

vacillations per 1000 committed branches. Define the *overlap ratio* to be the total number of overlapping dynamic branches divided by the total number of committed dynamic branches. The *overlap vacillation ratio* is the total number of times a dynamic branch both overlaps and vacillates divided by the total number of overlapping dynamic branches. Each of these results are shown in Figure 6.9. The graph for vacillation rate is cut-off at the top for clarity because the art benchmark has an astounding vacillation rate of 160.

6.3.5 Flexible Update Schemes

To reduce delayed-update weakening as much as possible without causing significant amounts of shuffled-update weakening or incorrect-update weakening, several special-purpose predictors are developed that attempt to choose the best time to perform an update. Branches are either updated earlier than commit time to reduce delayed update weakening or updated at commit time to prevent vacillation from damaging branch prediction accuracy. These predictors, called *flexible update predictors*, can use any branch prediction technique.

Static branches may prefer one update method uniformly throughout execution. The first technique, *static*, chooses beforehand whether instances of a branch should update at resolve or commit time. It does this based on prior knowledge of the static branch prediction accuracies for both update methods. This information is gathered for each benchmark in a training run. In this study, training is done with the full reference inputs of the benchmark set. Though training in this way is unrealistic, the predictor is mainly being used for analysis to reflect the best that a static flexible update predictor can do. Research in using smaller input sets to train the predictor is beyond the scope of this study.

If branch vacillation behavior turns out not to be uniform, a predictor must be designed that

can dynamically choose what update time is best. A second technique named *update chooser* is set up much like a hybrid predictor. There are two core predictor states identical in every way except that one always updates at resolve time and the other always updates at commit time. A 2-bit chooser table, similar to the hybrid chooser described in [McF93], is used to reference the more accurate predictor entry among the two states. The chooser table entry is updated at branch commit time. This predictor is the most direct of the three, but may easily be the largest since it requires an additional table for the chooser as well as a second BHT or PHT.

The final technique aims to dynamically find the best update time for branches based on whether or not the branch vacillates. A *vacillation predictor* dictates when the system predictor updates particular branches. By allowing updates for non-vacillating branches at resolve time while restricting vacillating branches to only update at commit time. It uses a *branch vacillation table*, or BVT, of saturating counters to keep per-branch vacillation information. The BVT has as many entries as the system predictor's BHT or PHT. It is indexed in the same manner as the BHT. When a vacillating branch commits, it is penalized by incrementing its BVT entry by some amount called the *vacillation penalty*. When a branch commits without vacillating, its entry is decremented. Upon branch resolve, the branch's predictor entry is updated if its BVT entry is below some set number called the *trust level*. If this happens, the branch is said to be *trusted*. A branch that isn't trusted must update its predictor only when it commits. To limit the number of experiments, the trust level is fixed at 1 and vacillation penalties are set to the maximum value that a BVT entry can hold. In test runs on the benchmarks using a hybrid predictor, BVT entries of 2 to 12 bits were tested and trends show that larger vacillation penalties yield higher branch prediction accuracies. The highest accuracies were attained when the predictor never trusted

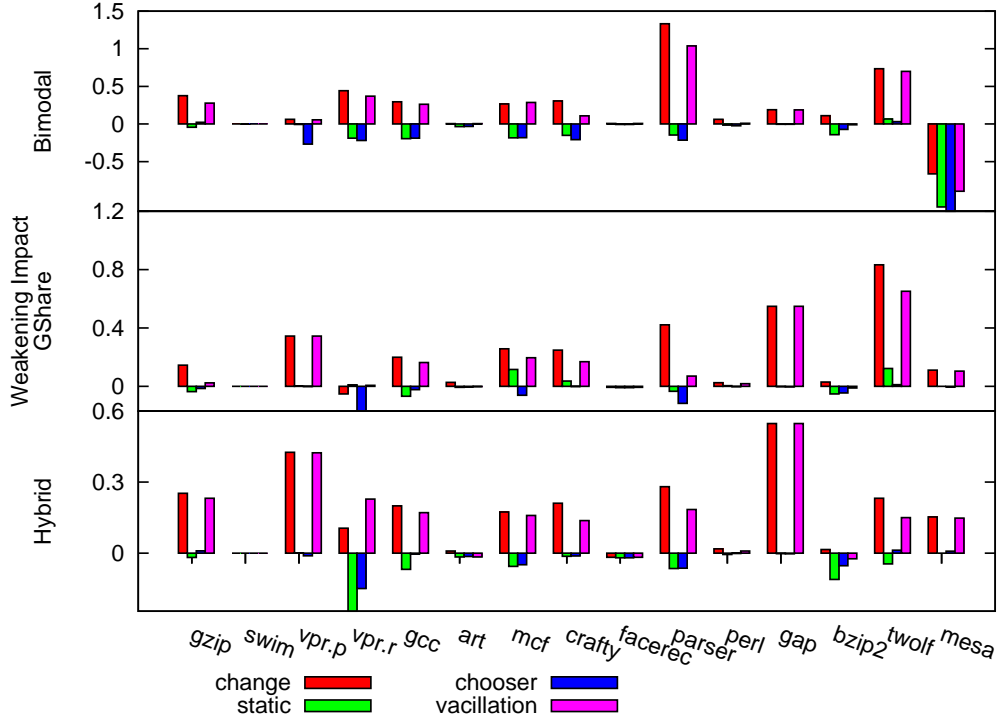


Figure 6.10: Misprediction Rate Impact of Flexible Update Schemes (petdis.90,103,104,106); Results are shown as the increase in misprediction rate from a system updating predictors at commit time.

vacillating branches. This is accomplished by using a 1 bit-per-entry BVT initialized to 0. If a branch vacillates, its BVT entry is set to 1 and it will not be trusted for the rest of execution. This is the way in which the vacillating predictor used in this study is configured.

6.3.6 Performance of Flexible Update Schemes

Each of the proposed techniques was simulated on a static sniper system. The results for each flexible update method with bimodal, GShare, and hybrid predictors are shown in Figure 6.10. Results are presented as the increase in misprediction rate from updating at commit time, and updating at **change** has been added for comparison.

For the bimodal predictor, almost all benchmarks favor the **commit** update method over **change**.

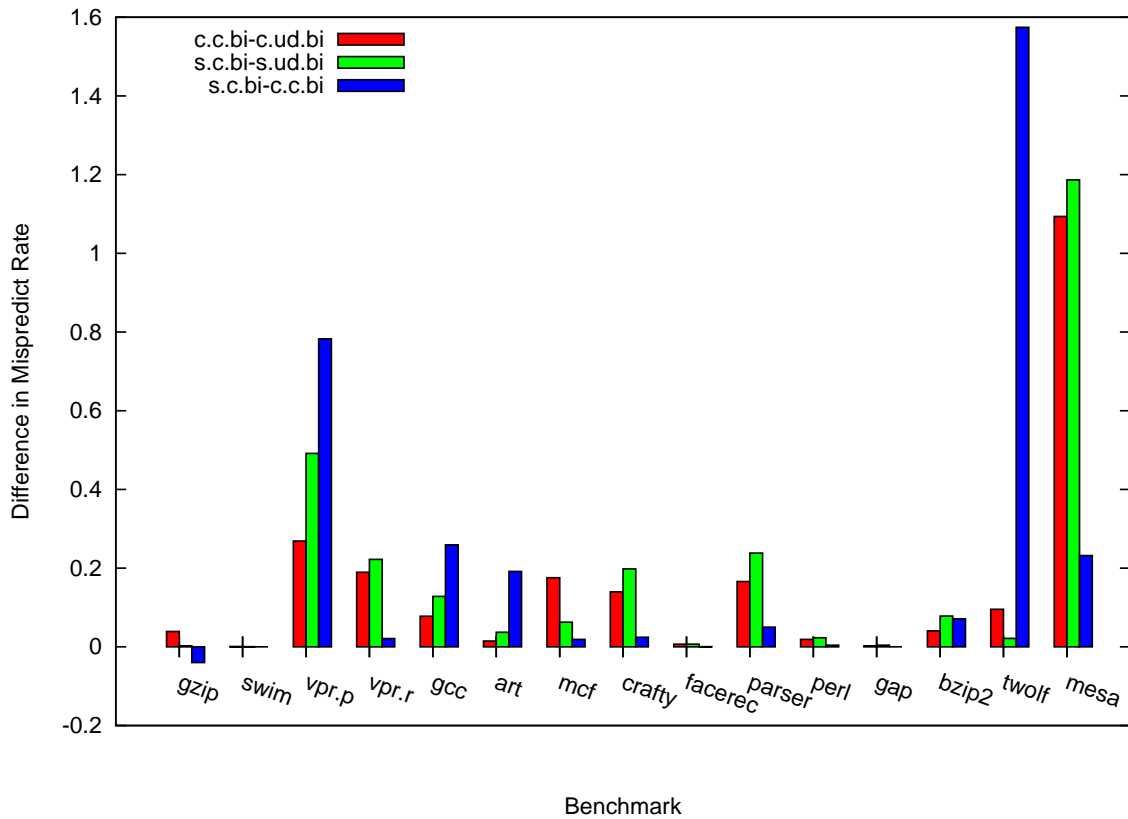


Figure 6.11: Analysis of Bimodal Chooser (petdis.90,111); Results shown as differences in misprediction rates of several systems.

The static and chooser flexible update techniques perform better than the base sniper system, reducing the misprediction rate by around 0.2. The vacillation predictor does not perform better than the regular system predictor.

Precisely answering the question of how much delayed update weakening can be avoided is difficult when examining the behavior of correlating predictors because they are affected by mangled-path weakening as well. Recall that the only type of weakening that affects systems with bimodal predictors is delayed-update weakening. Because it performs best, the amount of weakening that the flexible update chooser can reduce will now be analyzed in detail.

Call a conventional system that uses a bimodal predictor that updates at commit *c.c.bi* and

the same system that uses a bimodal update chooser predictor $c.ud.bi$. Call a sniper system that uses a bimodal predictor that updates at commit $s.c.bi$ and one that uses a bimodal update chooser $s.ud.bi$. The improvement of the misprediction rate for the bimodal chooser on a conventional system is $R^{c.c.bi} - R^{c.ud.bi}$. Likewise, the improvement for a sniper system is $R^{s.c.bi} - R^{s.ud.bi}$. The bimodal weakening impact is $R^{s.c.bi} - R^{c.c.bi}$. These three differences are represented in Figure 6.11 by the first, second, and third results for each benchmark respectively.

The first result in the figure shows that even a conventional system benefits from the chooser flexible update predictor. Among the benchmarks that benefit are the ones most affected by update lag in the bimodal predictor in Figure 6.5. Sniper benefits more from the update chooser than the conventional system, as shown by 11 of the 15 benchmarks. The difference between the first two results is a reasonable measurement of the amount of alleviated delayed-update weakening. Compare this difference to the last result, which shows the total weakening. In four cases, *vpr.place*, *vpr.route*, *crafty*, and *parser*, the update chooser alleviated almost all weakening. In 4 benchmarks there were more minor reductions in weakening.

Because it cannot be easily isolated from mangled-update weakening, it is not as easy to measure the amount of alleviated delayed-update weakening for GShare and hybrid predictors. However, a good estimation can be provided using the classification of Figure 6.3. Towards the end of the study, when providing results for a CIP-aware predictor, this estimated measurement will be presented.

6.4 Mangled-Path Weakening

6.4.1 Description

Since true CDR outcomes are not known to post-reconvergent branches until after prior protected branches resolve, it is impossible to obtain a correct GHR to predict CI instructions in a CIP. Mangled path weakening is weakening caused by differences in paths from a conventional system to a CIP.

Call the bits in a GHR corresponding to the CDR the *padded region*. In a conventional system the padded region would consist of the correct outcomes of the CDR branches. In a CIP they are at best a guess, and so mangle the GHR. There are two ways in which a CIP mangles the GHR. First, the number of outcome history bits in the padded region, called the *pad size*, may not match the number of branches in the correct CDR. If the padded region is too small, noise may be brought in at the fringe and cause branch predictor training time to increase. If it's too large, useful correlation data could be pushed out at the fringe and cause weakening due to lack of correlation data. The other way in which the GHR is mangled is the contents of the padded region. Since the true CDR outcomes cannot be used, *outcome history padding* schemes that inject false histories into the path at special times in execution are used. A common technique involves padding with predicted CDR outcomes, even though they may be incorrect. This provides a best guess, but may not be the best way to minimize weakening.

Define *fringe noise ingestion* to occur when noisy branch outcomes are brought into the global history that would otherwise not appear on a conventional system. *Fringe signal loss* occurs when useful data is pushed out of the GHR. Define *CDR signal loss* to occur when the padded region lacks important correlation data it would otherwise have in a conventional system. Finally,

CDR noise ingestion occurs when incorrect CDR outcomes not containing valuable correlation data cause weakening. These are the causes of mangled-path weakening.

A dynamic CIP can turn protection on and off and therefore change the padded region from the correct CDR outcomes to predicted CDR outcome bits, or even to no bits at all. Consider a dynamic CIP that does not put outcomes in the padded region when protecting a branch. If protection of the branch turns on and off during execution, subsequent branches may suffer from all the afore mentioned types of mangled-path weakening. A static CIP that does not include outcomes in its padded region can only suffer from fringe noise ingestion and CDR signal loss.

The weakening that fringe noise ingestion causes is referred to as *external insulated weakening*. Likewise, fringe signal loss causes *soft absentee weakening*, CDR signal loss causes *hard absentee weakening*, and CDR noise ingestion causes *internal insulated weakening*. Recall, since true CDR outcomes are simply not available when protecting a branch in a CIP, hard absentee weakening cannot be avoided.

6.4.2 Examples

On a system using GShare, the branch at address 0x1a950 from the SPEC CPU 2000 benchmark crafty is a simple yet effective example of internal insulated weakening. The branch's misprediction rate rises by 10% when using snippet. Throughout the majority of execution, the branch is highly biased not-taken. Observation of the system state shows that the branch's GHR often contains outcomes from misspeculated paths at predict time. This causes the branch to be associated with more table entries and hence exhibit a longer training time.

A system with a Hybrid predictor is used in the following example. In the art benchmark, the branch at address 0x12fbc is the top weakened branch of the benchmark, doubling in mis-

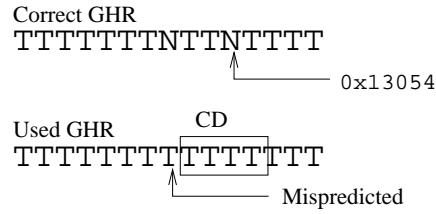


Figure 6.12: GHR State for Branch 0x12fbc

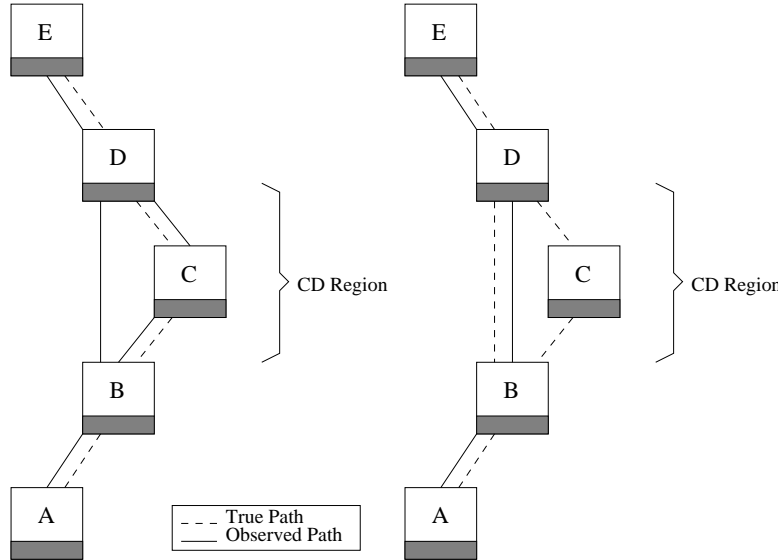


Figure 6.13: Control Flow Graphs of Two Separate Executions

predictions when using snipper. In areas of execution, the branch exhibits a very stable local history of TTTTTTTTTTN continuously. The GHR is too small to reflect this entire pattern with nearby global outcomes; however, this branch is highly correlated to another branch at address 0x13054. Figure 6.12 shows that the correct outcome of the correlated branch is not reflected in the GHR when using Snipper, since the CD path taken does not contain it. This exemplifies one case of hard absentee weakening in which a branch is weakened when correlation data within the CD region is unavailable due to a misprediction of the incident branch.

6.4.3 Path Splitting and Joining

Because CIPs fetch out of program order, observed paths of correlating predictors may not necessarily be true paths. Refer to the first control flow graph of Figure 6.13 which shows a control flow graph of a certain area in a program leading to the basic block A . Only the basic blocks of paths leading to A are shown. Assume that the branch in B is highly correlated to the one in D and that D has been marked for protection. The true paths are marked along with observed paths in a CIP. Assume that a conventional system will always fetch A through the control path $EDCB$. Notice that there are two ways in which the CIP fetches A , $EDCB$ and EDB . The latter is not a true path yet is still an observed path containing the CD region where the protected branch D is mispredicted.

If the branch predictor of a CIP uses predicted CDR branch outcomes for the GHR's padded region, both control paths EDB and $EDCB$ are observable from A even though only one of them is a true path. This is an example of how paths may be *split*. Since each path corresponds to a PHT entry and each entry requires some amount of training, splitting paths typically increases the training time of branches.

Paths may also be *joined*. The second control flow graph in Figure 6.13 shows two possible true paths through the region. Assume that in this case the branch in B is no longer correlated to the one in D . A conventional system will observe both of these control paths, $EDCB$ and EDB , in execution. A CIP that does not include CD data in its path, however, will only observe one path through this region. This is an example of how paths may be joined.

Define the union \cup of two path filtered local histories, L_1 and L_2 , to be the combined local history of the paths' outcomes arranged in program order. Consider two systems, X and Y . A

path-filtered local history on system X , L^X , is said to be *perfectly split* into L_i^Y , for all $0 \leq i < n$ for some integer n , such that the following holds.

$$\text{Perfect Path Splitting: } L^X = \bigcup_{0 \leq i < n} L_i^Y \quad (6.6)$$

Path filtered local histories L_i^X , for all $0 \leq i < n$ are said to be *perfectly joined* if there exists a path filtered local history L^Y on system Y such that the following holds.

$$\text{Perfect Path Joining: } L^Y = \bigcup_{0 \leq i < n} L_i^X \quad (6.7)$$

Realistically, perfect path splitting is expected to happen rarely. A more common case is when a path filtered local history splits into paths that contain outcomes from other paths.

$$\text{Path Splitting: } L^X \subseteq \bigcup_{0 \leq i < n} L_i^Y \quad (6.8)$$

To avoid overcomplicated analysis, only the perfect path joining and perfect path splitting models are discussed for the remainder of this chapter. It is realized, however, that this is not always the case.

Figure 6.14 shows examples of how paths may split or joined. The horizontal lines denote the bias of the path filtered local history with respect to time. A higher line indicates a taken outcome while a lower line indicates a not-taken outcome. The outcomes are marked for each point in time the branch reached by the path resolves. The shaded region denotes an inevitable misprediction. Assume that the update lag is low enough such that there are no delayed update mispredictions

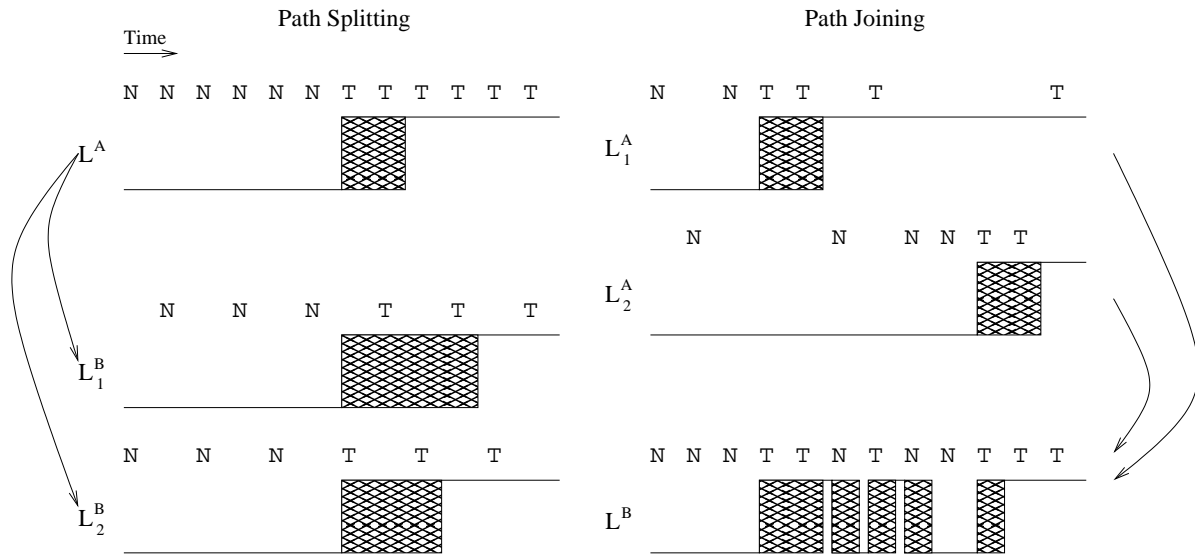


Figure 6.14: Examples of Path Splitting and Joining

and assume no predictor collisions.

The left side of the figure shows how a path may be split from one system to another. The bistable path above the line is split into the two separate bistable paths shown below the line. Note that the amount of mispredictions go from two to four. The right side of the figure shows how two bistable paths in one system may be joined in another system. Since the bias of the two shown paths are usually not similar, the number of mispredictions rises substantially when the paths are joined. The different causes of path splitting and joining will be articulated as well as some performance implications for each.

Thus far, it has been shown how path splitting and joining can hurt performance, but this is not always the case. Consider two separate paths of a conventional system, both highly biased taken. Each path suffers two training mispredictions since they each have a separate predictor entry to train. If the path in some system is modified to join these two original paths so that they share a PHT entry, then the amount of training mispredictions is halved. This example shows that

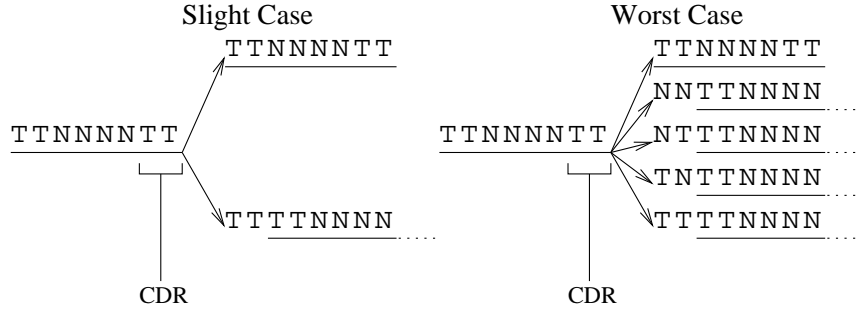


Figure 6.15: Examples of External Insulated Weakening

even conventional systems may benefit from modification of the way the PHT is indexed, though studying this in detail is beyond the scope of the thesis.

Causes of Mangled Path Weakening

All proposed CIPs either predict post-reconvergent branches using the predicted CDR outcomes or completely leave these outcomes out of the GHR. To exemplify the different types of mangled path weakening, first consider a CIP that leaves CDR data out of the path. The GHR samples marked *Slight Case* in Figure 6.15 show the GHR of one path for some post-reconvergent biased branch in a conventional system being split into two paths on a CIP. The first split path is observed when a candidate branch (whose outcome is the first in the marked CDR) is not protected yet. This path is identical to the true path of the conventional case. The last split path is that of the branch when it is a post-reconvergent region of some earlier protected branch that has yet to resolve. Notice that since the CDR outcomes are no longer present in the history (marked by a dotted underline), two more distant outcomes appear (not underlined). This is an example of fringe noise ingestion. The external insulated weakening in this case will be the added mispredictions for the training of this new path. The *Worst Case* example shows that ingestion of noisy branches can add a considerable amount of mispredictions. The two outcomes brought in at the fringe are noisy, and so the original path is split into four separate paths, each of which will suffer

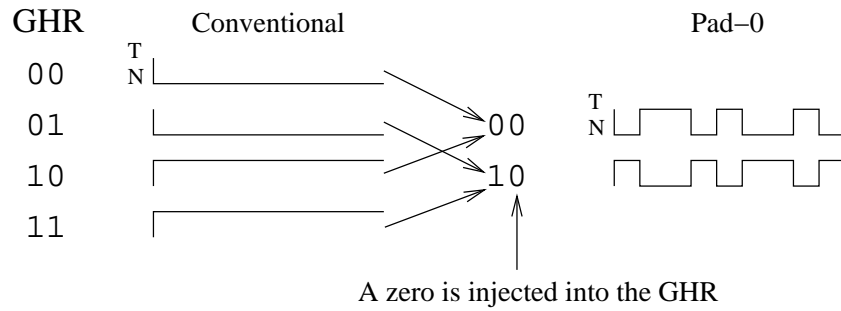


Figure 6.16: Push Displacement Causing Path Joining

the same amount of training mispredictions.

It has been established that noise ingestion causes weakening by splitting paths. Signal loss may also cause weakening, but not in the same manner. Figure 6.16 shows how a branch correlated to an outcome that is not available in a CIP can cause weakening via path joining. Assume a 2-bit GHR. The GHR values when predicting some branch B are shown in the first column of the figure. The second column shows the path filtered local histories for B on a conventional system. Clearly, B is correlated to a branch two instructions away. The third column shows the path filtered local histories in a CIP when padding with a 0 right before B is predicted. The correlated outcome has been pushed out and the branch is now observed on only two paths. Since a monostable taken path filtered local history is joined with a monostable not-taken one, the resulting path is now a lot more difficult to predict. This is an example of how signal loss can cause paths to join, causing absentee weakening. If the correlation data is lost and not in the padded region, the CIP can bring the signal back in using a different padding scheme. In this example the signal was lost at the fringe, but the same joining result holds when the signal is lost in the CDR.

The control flow graph shown in Figure 6.17(a) is expanded from one appearing earlier in this study. In the figure on the left, branch D is highly correlated to branch A, a difficult branch

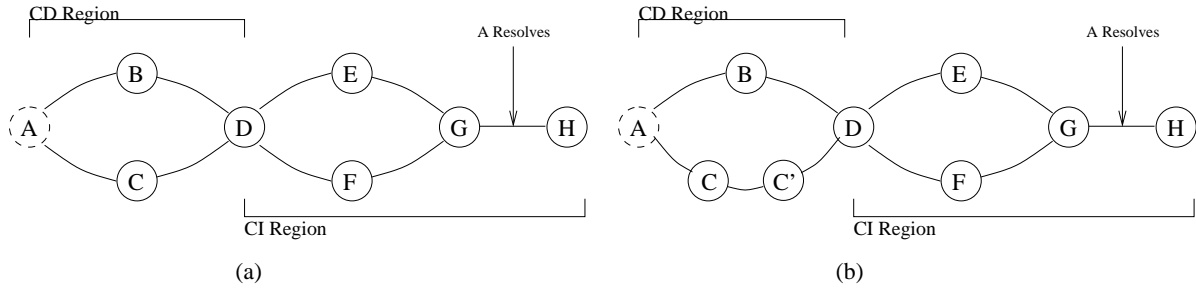


Figure 6.17: Control Flow Example for CDR Juggling

to predict. The branch H, a monostable branch, will be reached from two control paths in a conventional system, either ABDEG or ACDFG. As described before, H will be reached from two additional paths in a CIP that uses CDR outcomes to predict, ACDEG and ABDFG. Though there haven't been any outcomes pulled in or pushed out of the GHR, the incorrect CDR outcomes can still cause weakening since each of these paths needs to train in the predictor. This is an example of how noise ingestion in the CDR can cause internal insulated weakening.

Because different paths through the CDR may vary in the number of branches per path, internal insulated weakening may occur in tandem with soft absentee weakening or external insulated weakening. Figure 6.17(b) shows a CFG which adds another branch C' to one of the paths through the CDR. In a CIP, the control path ABDEG path is split into ABDEG and ACC'DEG. Since the latter path contains more outcomes than the true path, fringe signal loss, and hence soft absentee weakening, becomes possible. This shows that different types of mangled-path weakening may occur in tandem.

Since path splitting and joining can improve performance, the way in which CIPs mangle paths can help branch prediction accuracy. It is evident, however, that it usually hurts more than helps [HR07].

To help bring a general understanding to how a CIP changes true paths, certain path statistics

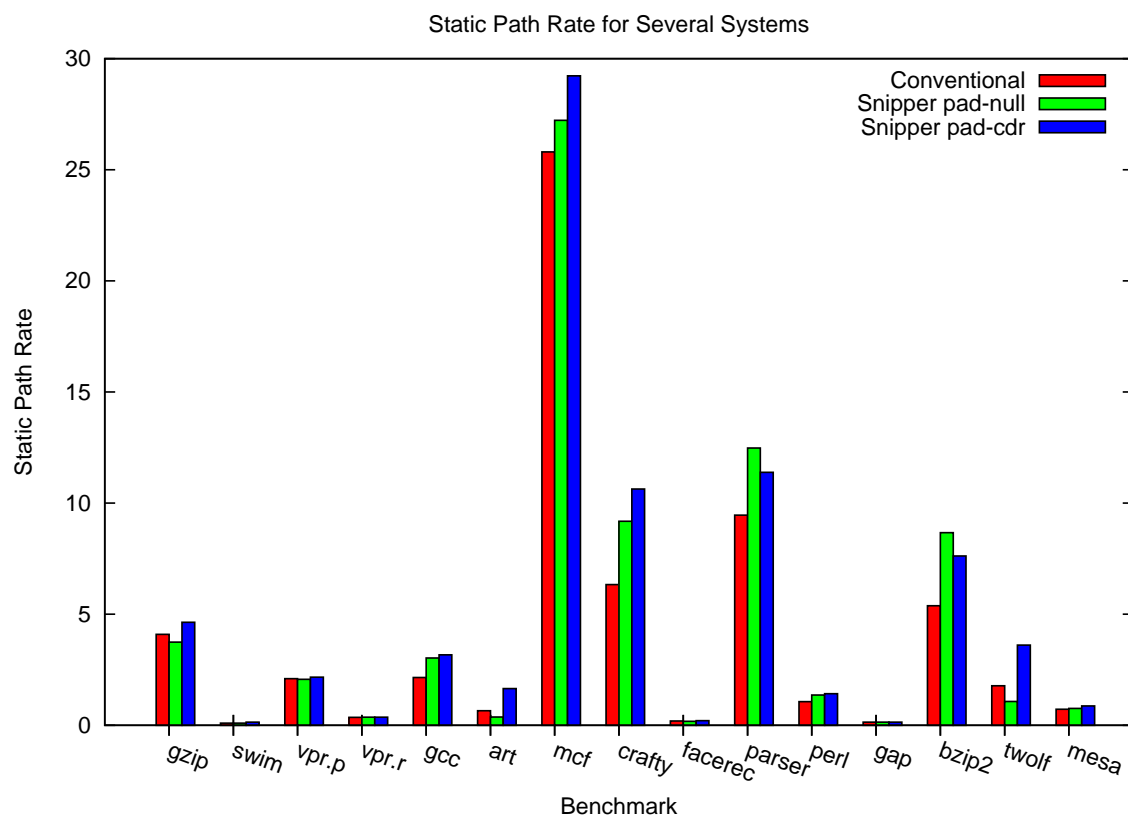


Figure 6.18: Static Path Rate for Several Systems (petdis.111)

are measured and evaluated. The results are gathered using a predictor that analyzes pure 16-bit paths and is collision-free. Define the *static path rate* as the total number of static paths seen in this configuration divided by the static instruction count. The division is performed to scale results better for clarity of Figure 6.18. Shown in the figure is the path rate for a conventional system, a sniper system that does not use outcome history padding (pad-null), and a sniper system that pads with predicted CDR outcomes (pad-cdr). Note that these path results are meant to give a quick look into sniper's behavior under different padding schemes. It is not intended to provide any major conclusions, since it does not reveal anything about the manner in which the static paths are used or branch prediction accuracy for the paths.

The results carry a notion that sniper, whether it's using pad-null or pad-cdr, tends to split paths. Extreme increases in the static path rate from the conventional system to sniper pad-null, like those of crafty, parser, and bzip, gives a clue that noise ingestion may be a factor (remember, this is static sniper). In almost every case, padding with the predicted CDR outcomes further increases the total number of static paths. The parser and bzip2 benchmarks actually have fewer static paths in sniper pad-cdr than sniper pad-null. These benchmarks seem to split paths by ingestion at the fringe much more than by ingestion in the CDR.

6.4.4 The Effect of Path Splitting and Path Joining

Path splitting and joining from a conventional system to a CIP have the potential of causing considerable amounts of weakening. To get a notion of how drastic the weakening could be, a model is developed that demonstrates simple cases of splitting and joining. Equations presented in this section assume no update lag.

Assume a path filtered local history with a constant number of outcomes per run. Assume the

number of outcomes per run is considerably large. Also assume that the initial PHT entry value, 0 or 3, will cause a misprediction, and that there are no collisions. Call the number of runs in the history ϕ . Let $L(i)$ represent the i 'th outcome of the path filtered local history L . Assume that history L^X is split into two paths, L_1^Y and L_2^Y such that any outcome $L^X(i)$ occurs in the new path $L_{\mathbb{S}(i)}^Y$, where \mathbb{S} models the way in which the path is split. Set \mathbb{S} to be a random variable representing a Bernoulli trial. This models a scenario near what the worst case split would be.

The number of mispredictions of the path filtered local history L^X is 2ϕ , since each run will have two training mispredictions. The number of mispredictions of each path L_1^Y and L_2^Y is also 2ϕ . The total number of mispredictions for the original path L^X doubled in the system where it has split. The weakening due to the modeled path splitting is then 2ϕ additional training mispredictions.

$$\text{Bistable path split : } W_{split}^{X,Y}(L) = M^X(L^X) \quad (6.9)$$

The model corresponds to some path in a conventional system that suffers from one bit of noise ingestion, where the noisy branch's outcome is random. This one unwanted bit in the GHR can cause a considerable amount of weakening, doubling the amount of training mispredictions for the original path. Indeed, the amount of mispredictions with respect to the amount of ingested noisy bits rises exponentially. Thankfully, the large majority of applications do not contain large amounts of noisy branches.

Assume two highly biased path filtered local histories L_1^X and L_2^X . Two cases are analyzed for the joining of two paths. For the first one, assume that paths L_1^X and L_2^X are each monostable unanimous. These paths are joined to form the history L^Y such that $L^Y(i)$ occurs in $L_{\mathbb{S}(i)}^X$ for all outcomes i . Here, the two monostable paths have joined into one monostable path. This causes

M^{L^Y} fewer mispredictions in the system Y .

For the second case, assume that L_1^X and L_2^X are monostable dissonant. Since the signals oppose each other, the joining of these paths causes a tremendous amount of weakening. Instead of using the Bernoulli trial to join the two paths, assume the paths will be joined by interdigitation so that $L^Y(i)$ is taken from $L_{i\%2}^X$. Joining the paths in this way will cause $i/2$ mispredictions.

$$\text{Monostable dissonant path join: } W_{join}^{X,Y}(L_1^X, L_2^X) = i/2 \quad (6.10)$$

Though the modeled cases for Equation 6.9 and Equation 6.10 probably do not happen often, they demonstrate near worst cases on the amount of weakening a path join or split may cause.

6.4.5 Outcome History Padding

Recall that since the padded region in a CIP can not consist of the correct CDR outcomes, the outcome history padding method becomes important. There are two main issues of CIPs that cause mangled path weakening. First, the size of the outcome history padding not matching the size of the conventional padded region. This may cause external insulated weakening and soft absentee weakening. The second issue deals with the contents of the padded region and may cause internal insulated weakening and hard absentee weakening. The following padding schemes are designed to address these issues.

One method mentioned several times in this study is *pad-null*. When using this method there is no outcome history used for padding. CDR outcomes are left out entirely and no false histories are injected. Using this padding method is favorable if there usually aren't noisy outcomes ingested at the fringe. This technique eliminates internal insulated weakening in static CIPs, though it may increase the amount of external insulated weakening in doing so.

Including predicted CDR outcome data is another method mentioned many times earlier in this study. It is referred to as *pad-cdr*. This method is the only one we present that may cause internal insulated weakening due to CDR juggling. However, post-reconvergent branches may attain higher accuracies when correlating to incorrect predicted CDR outcomes rather than nothing at all. Additionally, if the different paths through the CDR have a similar amount of branches, the padding size of this method could effectively prevent fringe effects.

A very simple padding scheme called *pad-0* is the one shown in Figure 6.16. Though it has a negative context in the figure, it has the potential to reduce weakening in CIPs by pushing noisy outcomes out of the fringe, which prevents path splitting. Padding similarly with two zero bits as opposed to one is called *pad-00*, and padding with three is called *pad-000*. The pad size can be customized for each static protected branch. *pad-0avg* uses the padding size for each protected branch as set by a profile. For our purposes, the profile sets the pad size to the average number of CDR outcomes for an entire reference input run of the branch's benchmark. This technique, called *fitted padding*, provides insight to how dynamically changing the padding size could help padding performance. Padding schemes that use it are suffixed with -avg. This naming convention is used for all the remaining padding methods. For this padding method and all remaining methods, the maximum static pad size is fixed at 3. This number has been chosen by examining the average number of branches in the CDRs of snipper-active benchmarks. This number ranges from 1 to 3.3, with the average being 2. Due to its potential complexity, study of changing the amount of padding bits for each protected branch beyond fitted padding is not studied here.

Padding with zeros may reduce mangled path weakening by removing noise from the fringe but

may cause unwanted path joining since it causes less variance across all paths. To prevent this, the *pad-c* method pads with the reconvergent branch's address bits instead of just zero bits. The bits are taken starting at the third least significant bit and going in the direction of more significance. For example, *pad-ccc* will pad the GHR with the third, fourth, and fifth least significant bits of the PC. This method allows post-reconvergent instructions to correlate with protected branches rather than their outcomes. The padding bits have been chosen intuitively to increase the chances that two nearby protected branches will pad with different values.

The *pad-cdr* method defined earlier differs from methods proposed so far in that it doesn't consistently use the same pad size for static protected branches in execution. If the number of branches in different CDR paths of the same static branch varies greatly, *pad-o* may be a better option. This method hashes the CDR outcomes to a constant pad size. Since some correlation data may be lost, some hashing algorithms may be more optimal than others. The hashing algorithm used for this study is fixed as the following.

```
s_cdr = number of branches in the CDR
s_pad = pad size
cdr[s_cdr] = sequence of CDR outcomes, index 0 is most recent
pad[s_pad] = 0
for i from 0 to (s_cdr DIV s_pad)
    pad = pad XOR cdr[i:i+s_pad]
```

The `:` operator in the pseudo code above represents a slice and indexing starts from 0. For example, `cdr[3:5]` is a 3-bit number consisting of the fourth, fifth, and sixth bits of `cdr` respectively. The padding size, number of branches in the CDR, and sequence of CDR outcomes are all given initially. After completion of the algorithm, the variable `pad` contains the padding. This algorithm was designed as a very simple approach. The padding is constructed by XORing consecutive segments of the CDR outcomes until all of them have been operated on. For the last

Table 6.2: Padding Methods

Name	Padding	Variations	Pad Size
pad-null	No padding	None	Fixed
pad-cdr	Predicted CDR outcomes	None	Variable
pad-0	0	pad-00, pad-000	Fixed
pad-0avg	0		Variable
pad-c	Reconvergent Branch's Address	pad-cc, pad-ccc	Fixed
pad-cavg	Reconvergent Branch's Address		Variable
pad-o	Hash of predicted CDR outcomes	pad-oo, pad-ooo	Fixed
pad-cavg	Hash of predicted CDR outcomes		Variable

segment, zeros are used as padding if there are not enough outcomes to fill the entire segment.

Table 6.2 shows a summary of all the different padding types explored in this study.

6.5 Performance of Outcome History Padding Schemes

All of the padding schemes presented above have been simulated and analyzed for each of the benchmarks. Of all three static padding sizes of those schemes with them, a padding size of 3 yields the best branch prediction ratio on average, followed by a padding size of 2, then 1. The fitted padding methods perform nearly as well as their 3-bit counterparts. The results for all the padding schemes of interest are shown in Figure 6.19 for GShare and Figure 6.20 for hybrid. For clarity, the results are shown as the increase in misprediction rate from the pad-null scheme. Graphs of collision rates are appended help give insight as to why some padding schemes are outperforming others.

The GShare predictor is generally more sensitive to the padding schemes than the hybrid predictor. The best case improvement in misprediction rate with GShare is about 0.7 whereas with hybrid it's nearly 0.2. Of all the benchmarks, twolf is the only one that responds negatively to the developed padding schemes, it performs best with pad-null. On average, the pad-ccc scheme outperforms the rest, with pad-cavg being a close second. The collision results appended to the

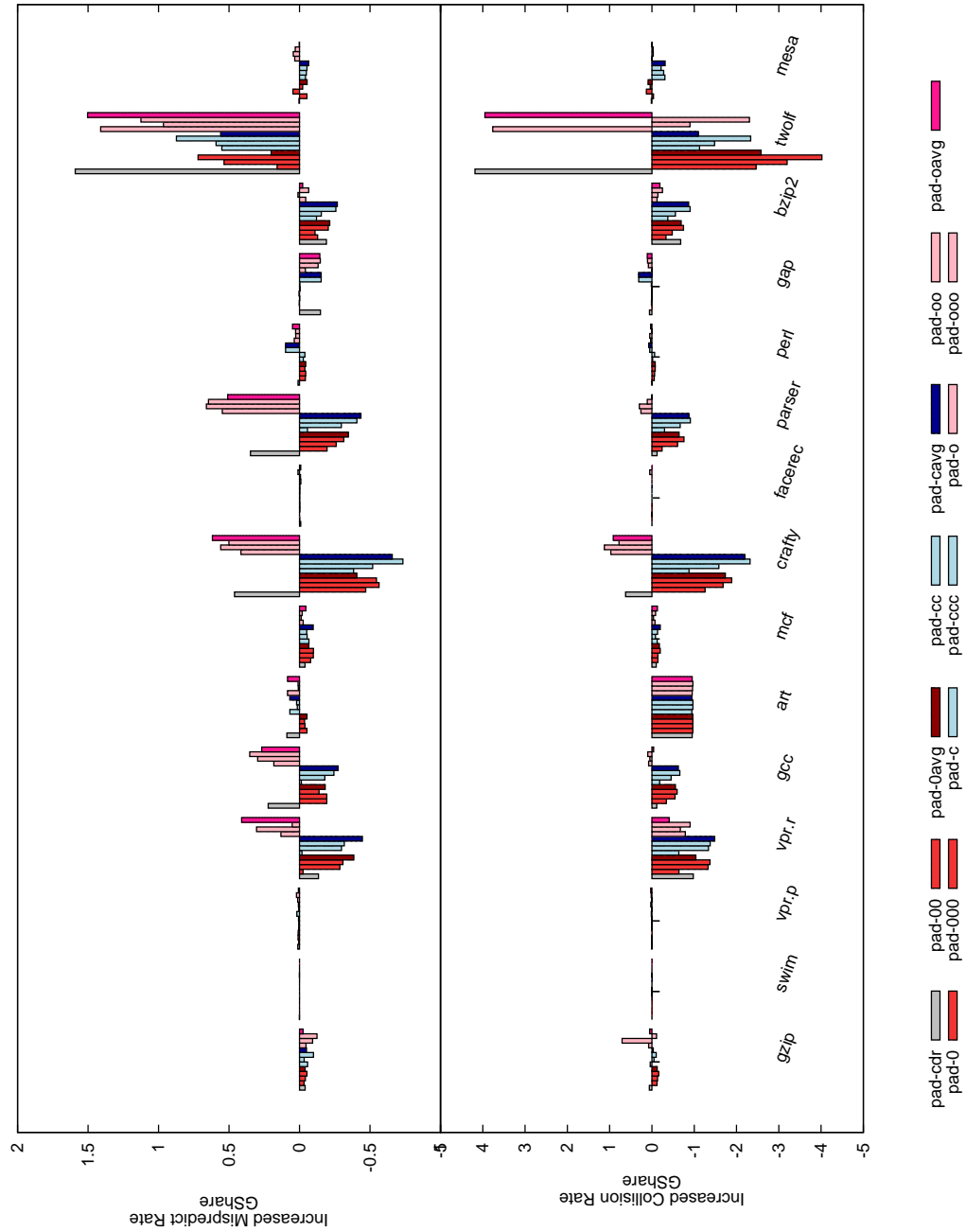


Figure 6.19: Misprediction Rate and Collision Impact of Padding Schemes for the GShare Predictor (petdis.137); Results are shown as the increase in misprediction rate from a system using pad-null.

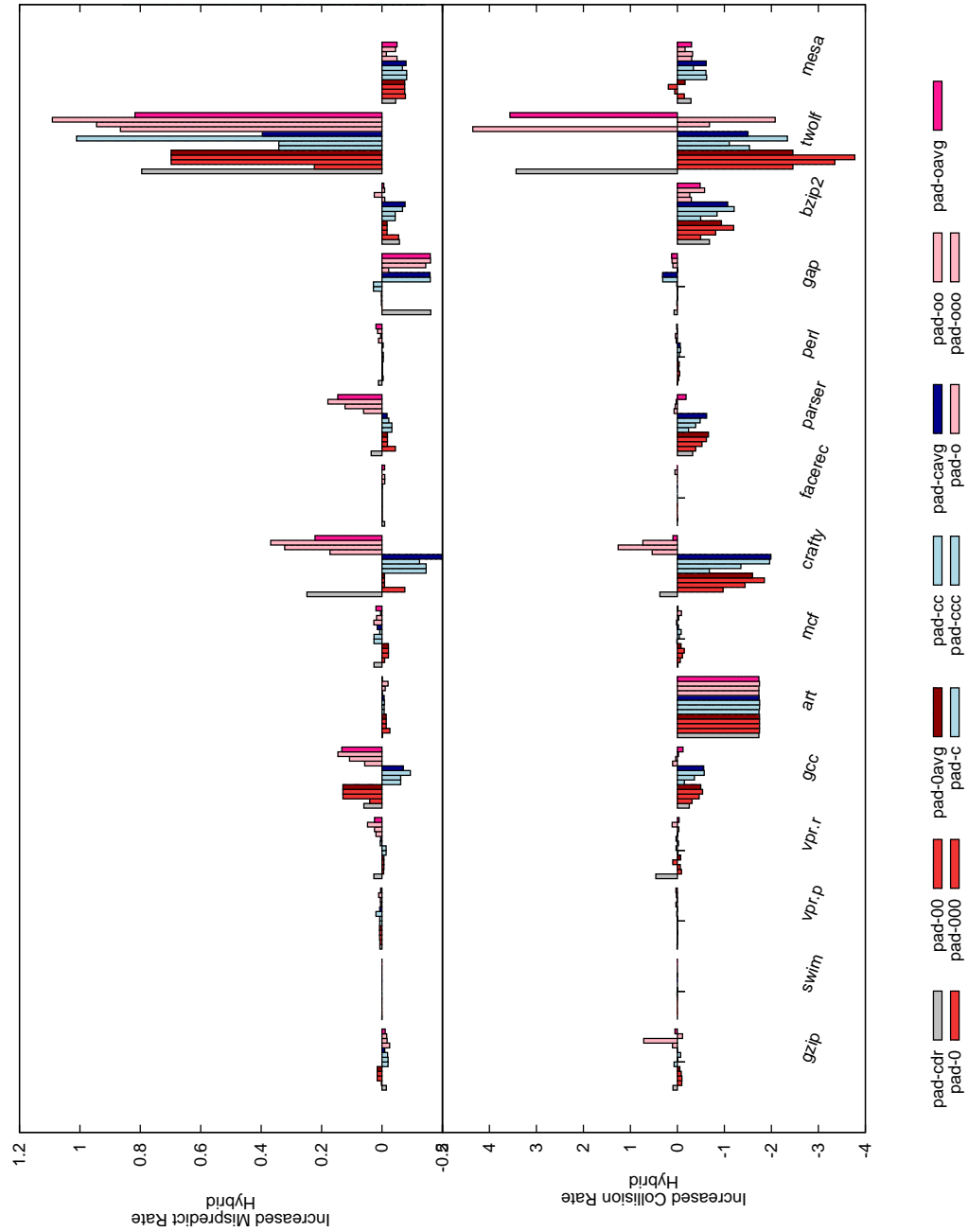


Figure 6.20: Misprediction Rate and Collision Impact of Padding Schemes for the Hybrid Predictor (petdis.137); Results are shown as the increase in misprediction rate from a system using pad-null.

graph give insight as to why this could be. Collision results for pad-c techniques are typically less than those of other techniques, especially pad-o which tends to drive the predictor to more collisions.

Chapter 7

Measurement by Weakening Type

The previous chapter formally defined several types of weakening. Here, techniques for measuring interesting subsets of the weakening types will be described. Measurement of weakening is important since it sheds light on where efforts in reducing weakening should be spent. Moreover, it helps assess how effective a reduction technique is for its targeted weakening type.

7.1 Approach

Finding the reason that a dynamic branch is weakened in the CIP is difficult, mainly because it's hard to isolate the outcomes to which a branch is correlated. A practical approach to classify weakened branches is to examine the performance of system pairs chosen so that only one or a few weakening types occur from one chosen system to the other. The estimated breakdown of weakening by type shown in Figure 6.3 is constructed in this way. For example, a static CIP using `pad-null` can be compared to another that uses `pad-cdr`. It has already been established that weakening from the former system to the latter is mainly internal insulated weakening, external insulated weakening, and soft absentee weakening, all of which can be improved by padding methods.

The first system in the *model system walk* will be a conventional system and the last will be a sniper system. Intermediate systems will be modeled to isolate desired subsets of weakening for each *step* in the walk. The weakening from one step to the next will then be a measurement of some subset of weakening, and the sum of the weakening of every step will be the total weakening when going from a conventional system to a sniper system. Keep in mind that the intermediate

modeled systems may not be useful other than to collect this information.

Though measuring each weakening type is difficult, the systems were able to be modeled such that important subsets of weakening are measured. The targeted weakening types are as follows. In the study of mangled-update weakening earlier in the text, it was established that systems with a bimodal predictor mainly suffered from delayed-update weakening when predictors update at commit. Because it has not been measured for GShare and hybrid predictors, the first targeted weakening subset is delayed update weakening. To find the amount of weakening that is unavoidable when performing protected recovery, the second subset is hard absentee weakening. Other types of weakening presented here may be remedied by outcome history padding schemes, so soft absentee weakening, internal insulated weakening, and external insulated weakening comprise the last targeted subset. A way to measure each of these three types of weakening individually has not yet been developed.

7.2 Model Systems

Each modeled system of the walk is named with a tuple in which components are separated by a dot. The first item of the tuple indicates the type of execution, either conventional (c) or sniper (s), while the second indicates the type of padding. The model systems use a 64ki-entry hybrid predictor. The other parameters of the model systems' configuration meet those shown in Table 5.1.

The first system, *c.cdr*, is a conventional system.

The second, *c.o*, sets the padded region to a hash of true outcomes (in the same manner as pad-o) but there is no protected recovery. Because post-reconvergent branches are squashed on a protected misprediction, there is no re-execution for post-reconvergent instructions. This

eliminates nearly all of the update lag that sniper induces. Upon protecting a branch, this system pads the GHR with a hash of true CDR outcomes when it reaches the reconvergence point. In order to provide as much correlation data as possible, the pad size is customized to each static protected branch using fitted padding. This technique is used so that branches with larger CDRs are less likely to lose CDR correlation data in the hash. The purpose of the *c.o* system is to make CDR outcomes available for the protected branch's post-reconvergent instructions while padding with a consistent number of bits. Since there should only be a small amount of hard absentee weakening (because most CDR outcomes will be available in the pad) and no delayed update weakening (because there is no speculative execution), the weakening $W^{c.cdr,c.o}$ is predominantly due to external insulated weakening and soft absentee weakening.

The system *c.c* is similar to *c.o* except that the GHR is padded with PC bits (like *pad-cavg*) as opposed to true CDR outcomes. The pad size for each protected branch matches exactly to that of the *c.o* system. This way, there is no insulated weakening or soft absentee weakening between the two systems. The weakening $W^{c.o,c.c}$ is therefore due to hard absentee weakening.

The next system, *s.c*, uses sniper to perform protected recoveries. This means that the post-reconvergent instructions will be predicted earlier relative to the predicted branch that causes delayed-update weakening. The padding scheme is exactly the same as that of *c.c*. Therefore, $W^{c.c,s.c}$ is due to delayed-update weakening.

The final system, *s.null*, is a sniper system that uses the *pad-null* method. Because the system does not insert outcomes into the padded region, $W^{s.c,s.null}$ is due to fringe noise ingestion.

A summary of the modeled systems are listed as follows along with the behavior of Post-Reconvergent Branches (PRBs).

c.cdr: PRBs use true path and do not execute speculatively.

c.o: PRBs have access to most correct CDR outcomes, do not execute speculatively, and are reached by slightly mangled paths.

c.c: PRBs do not have access to CDR outcomes, do not execute speculatively, and are reached by slightly mangled paths.

s.c: PRBs do not have access to CDR outcomes, execute speculatively, and are reached by slightly mangled paths.

s.null: PRBs do not have access to CDR outcomes, execute speculatively, and are reached by mangled paths.

This classification is by no means presented as a be-all end-all measurement. On the contrary, this is only the first measurement of the presented weakening types and there may be plenty of room for improvement. Weakening measured by some pairs are expected to be more accurate than others. As mentioned before, $W^{c.cdr,c.o}$ may contain small amounts of hard absentee weakening, as outcomes may be lost in the hash. The hashing algorithm used may not be the best to prevent outcomes from being lost. Since there may be small amounts of absentee weakening in $W^{c.cdr,c.o}$, the measurement of hard absentee weakening, $W^{c.o,c.c}$, may not cover the actual absentee weakening of the system. The measurement of delayed-update weakening is expected to be fairly accurate, since there is only very little protection overhead in the c.c system it behaves much like a conventional one as far as predictor update timings are concerned.

7.3 Results

The results in Figure 7.1 show the weakening for each step of the model system walk from a conventional system to a pad-null sniper system. Note that the weakening is negative for some system pairs. Recall from earlier in the text that many of the behaviors that generally cause weakening may increase branch prediction accuracy in some cases. As the figure shows, this phenomenon is rare and is of very little magnitude when it does occur in most cases.

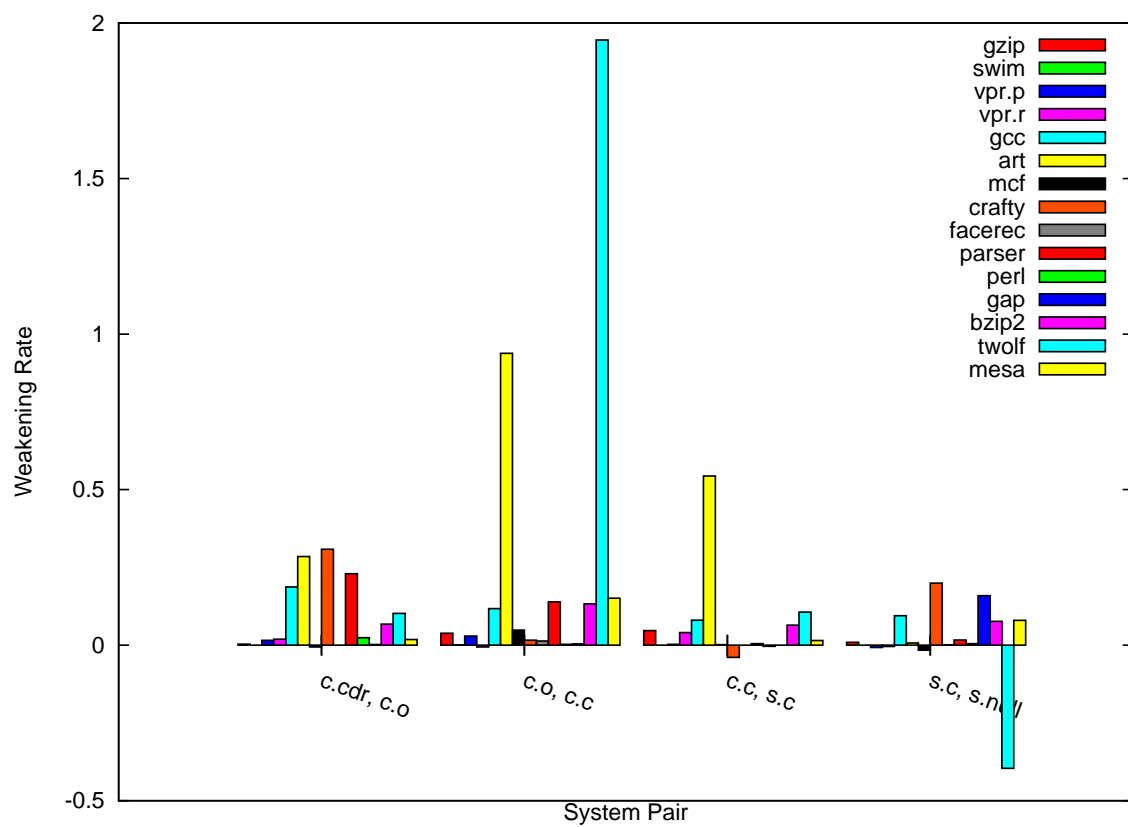


Figure 7.1: Weakening Among Model Systems (petdis.109)

The classification of Figure 6.3 was generated in the following way. Delayed update weakening is $W^{c.c,s.c}$, hard absentee weakening is $W^{c.o,c.c}$, and soft absentee and external insulated weakening are $W^{c.cdr,c.o} + W^{c.c,s.null}$. These classes are marked as mangled update, mangled path, and absentee in the figure. Some of these classes of weakening were measured as negative. This is expected since, as discussed earlier, the effects that cause weakening can also increase branch prediction accuracy. In generating the classification, these negative weakening results are factored out of the final percentage.

Chapter 8

CI Aware Branch Predictor

The majority of branch weakening is from CIP side-effects that may be reduced by using special branch predictor techniques. It has been shown that flexible update schemes can reduce significant amounts of delayed-update weakening for a CIP using the bimodal predictor while outcome history padding can improve branch prediction accuracy in the CIP. Now, the first CI Aware branch Predictor, or CIAP (pronounced *chap*), is presented. It will be implemented based on the presented weakening alleviation techniques based on their performance and ease of implementation.

8.1 Implementation

The branch predictor is designed to use the flexible update chooser and pad-ccc outcome history padding scheme with the hybrid predictor as a core. Since this study does not consider the cost of predictor size, enabling the flexible update chooser will cause the predictor to more than double the size of its Hybrid counterpart. In order to compensate for this cost, results are compared against conventional systems with a hybrid flexible update chooser. Outcome history padding has a relatively low cost on the design.

The CIAP with a Hybrid core will use two PHTs, two BHTs, and one chooser table, all of which have 2-bit entries. One hybrid predictor *state*, consisting of a PHT, BHT, and chooser, will update at change while the other will update at commit. A chooser, which is always updated at commit time, will choose one state just as described in Section 6.3.5. The predictor is configured to have 64ki entries and use a 16-bit GHR.

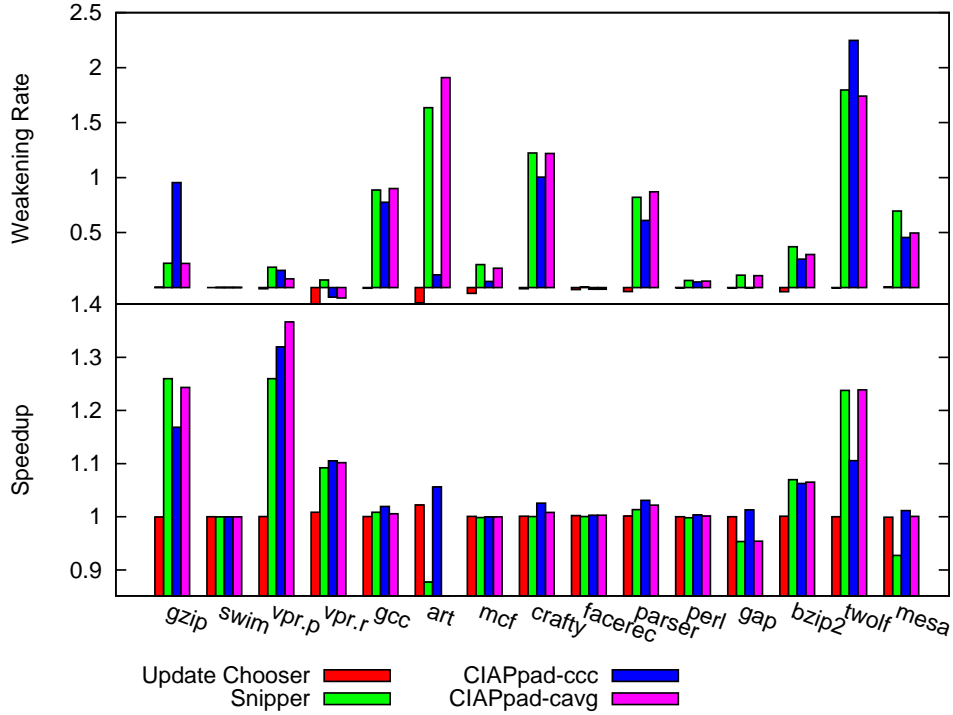


Figure 8.1: Performance of Hybrid CIAP (petdis.123); Results are shown as the increase in weakening rate and speedup from a conventional system with a hybrid predictor. The sniper system shown uses pad-null.

8.2 Results

A breakdown of the speedup and weakening rate results of several systems including sniper with the CIAP are shown in Figure 8.1. Note, all of the results in this particular figure are captured for dynamic sniper. Weakening results are measured from a conventional system with a regular hybrid predictor to the respective system labeled in the figure. The first result shows the weakening rate and speedup for a conventional system outfitted with an update chooser. The performance is expected to slightly increase in this case, but not dramatically since conventional systems are less susceptible to update lag. The second result is for a sniper system. The system is configured with pad-null for outcome history padding and a regular hybrid predictor that updates at commit

time. The third result is for sniper with the CIAP described earlier in the chapter, referred to as CIAPpad-ccc. A CIAP predictor that uses pad-c with fitted padding called CIAPpad-cavg has been added as the last result to provide a slightly more complex CIAP for comparison.

The flexible update predictor significantly improves the conventional branch prediction accuracy in the conventional case for 5 out of the 15 benchmarks. In only two of these benchmarks does this value equal the improvement in branch prediction accuracy from a sniper system to the CIAP system, meaning flexible update has helped eliminate some mangled-update weakening.

The CIAPpad-ccc predictor reduced weakening for 12 of the 15 benchmarks. The CIAP was able to reduce weakening enough to cause 3 benchmarks originally slowed down by sniper to exhibit speedup.

Of the 3 benchmarks that benefit greatly from sniper, 2 suffer more weakening using the CIAPpad-ccc as opposed to using a hybrid predictor with pad-null. Both of these benchmarks, gzip and twolf, do not react well to any of the weakening reduction techniques presented in this study. However, in both of these cases CIAPpad-cavg predictor maintains speedup very close to that of sniper. CIAPpad-cavg outperforms CIAPpad-ccc in 4 of the benchmarks, and performs nearly as well in most others.

Even with the unfavorable results of gzip and twolf, both CIAP predictors improve speedup and reduce weakening on average across all of the benchmarks. The CIAPpad-ccc improves speedup by 0.015 and reduces the weakening rate by $0.114\text{misp}/kI$. The CIAPpad-cavg improves speedup by 0.019 and reduces the weakening rate by $0.022\text{misp}/kI$.

To find the different types of weakening the CIAP has eliminated, refer to Figure 8.2. This is the measurement of weakening presented in the previous chapter for sniper outfitted with

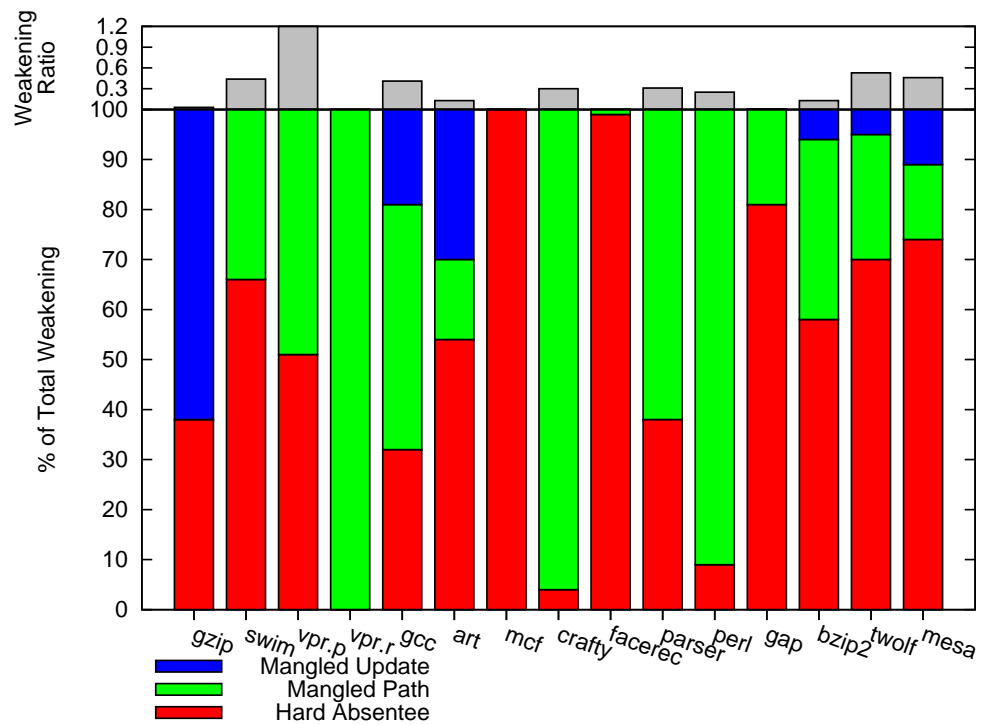


Figure 8.2: Weakening Classified by Type for Snipper with CIAP (petdis.131)

CIAPpad-ccc. Comparing this figure with Figure 6.3, the measurement shows that mangled-update weakening has been eliminated completely in 4 benchmarks that originally suffered from it in a snipper system with a hybrid predictor and the pad-null scheme. Mangled-path weakening has either been eliminated or greatly reduced in three of the benchmarks.

Chapter 9

Conclusion and Future Work

Branch weakening has been formalized and defined by its several causes. In doing so, this study has revealed that some types of weakening may be eliminated while others are inherent to control independence and cannot be avoided. Study of branch behaviors and branch predictors in both conventional systems and control independence processors enabled a thorough understanding of why branches are weakened. Through development of a classification that measures the several types of weakening, it has been established that the majority of weakening may be remedied by using special branch prediction techniques that reduce update lag and path mangling. Among the techniques that work best and are easy to implement, the CIAP has been introduced. This branch predictor uses fundamental weakening reduction techniques to eliminate weakening and does so successfully. Of all 15 benchmarks, 12 exhibited less weakening. Three benchmarks that were originally slowed down by sniper using a hybrid predictor and the pad-null method exhibit speedup with the CIAP.

The techniques used to reduce weakening that are presented in this study are among the most fundamental. Though a considerable amount of weakening has been reduced using these techniques, there is opportunity to explore more robust techniques and examine a larger parameter space.

Internal absentee weakening cannot be avoided when the branch inducing the weakening is marked for protection. Many current CIPs including sniper dynamically turn protection on and off in execution, but none of them consider this type of weakening when doing so. Detection of

a weakened branch in execution is feasible. A second predictor state that predicts and updates its GHR and tables at commit time can be used to compare against the system predictor. This *commit-time predictor* is not useful for predicting branches (since it predicts them too late), but can be used to detect weakening since it operates very similarly to a predictor in a conventional system. If the system predictor mispredicts a branch and the commit-time predictor yields a correct prediction, the branch instance may be marked as weakened. Though not discussed in this paper, a commit-time predictor has been used in this research to find examples of weakened branches for study. Though using this technique is a good way to dynamically detect weakened branches, finding the protected recovery that caused the weakening is a hard problem and has not been explored.

The mangled-path weakening reduction techniques offered in this thesis may be greatly improved upon. In many cases the pad-avg techniques show that one padding size certainly does not fit all. Padding schemes where the padding size dynamically changes in execution is not explored in great detail here, but is a good problem for future research since the results of the CIAP show that there is a lot of mangled-path weakening to be dealt with.

Because the base system of study used here updates at commit time, update shuffling and incorrect update have not been studied in detail. Though employing the CIAP eliminates delayed-update weakening for most benchmarks, it does so with a very aggressive technique that doubles predictor size. The vacillation predictor has a large parameter space could be explored much more rigorously in a more focused study.

Finally, techniques in classification can be developed for each distinctive type of weakening. Also, dynamic classification techniques may be developed in the future that classify weakened

branch mispredictions on the fly as opposed to using the postmortem model system approach. This could allow for greater performance by employing particular weakening reduction techniques to particular situations.

Bibliography

- [ARM] Arm8. <http://infocenter.arm.com/help/index.jsp>.
- [AZRRA07] Ahmed S. Al-Zawawi, Vimal K. Reddy, Eric Rotenberg, and Haitham H. Akkary. Transparent control independence (tci). *SIGARCH Comput. Archit. News*, 35(2):448–459, 2007.
- [CFS99] Yuan Chou, Jason Fung, and John Paul Shen. Reducing branch misprediction penalties via dynamic control independence detection. In *ICS '99: Proceedings of the 13th international conference on Supercomputing*, pages 109–118, New York, NY, USA, 1999. ACM.
- [CPT08] Bumyong Choi, Leo Porter, and Dean M. Tullsen. Accurate branch prediction for short threads. In *ASPLOS XIII: Proceedings of the 13th international conference on Architectural support for programming languages and operating systems*, pages 125–134, New York, NY, USA, 2008. ACM.
- [CTW04] Jamison D. Collins, Dean M. Tullsen, and Hong Wang. Control flow optimization via dynamic reconvergence prediction. In *MICRO 37: Proceedings of the 37th annual IEEE/ACM International Symposium on Microarchitecture*, pages 129–140, Washington, DC, USA, 2004. IEEE Computer Society.
- [CV01] Chen-Yong Cher and T. N. Vijaykumar. Skipper: a microarchitecture for exploiting control-flow independence. In *MICRO 34: Proceedings of the 34th annual ACM/IEEE international symposium on Microarchitecture*, pages 4–15, Washington, DC, USA, 2001. IEEE Computer Society.
- [DR95] Kaivalya Dixit and Jeff Reilly. Spec95 questions and answers. *SPEC Newsletter*, 7(3):7–11, 1995.
- [EM98] A. N. Eden and T. Mudge. The yags branch prediction scheme. In *MICRO 31: Proceedings of the 31st annual ACM/IEEE international symposium on Microarchitecture*, pages 69–77, Los Alamitos, CA, USA, 1998. IEEE Computer Society Press.
- [FRB01] Brian Fields, Shai Rubin, and Rastislav Bodk. Focusing processor policies via critical-path prediction. In *In Proceedings of the 28th Annual International Symposium on Computer Architecture*, pages 74–85, 2001.
- [GF00] Jayanth Gummaraju and Manoj Franklin. Branch prediction in multi-threaded processors. In *in Proceedings of the 2000 International Conference on Parallel Architectures and Compilation Techniques*, pages 179–188, 2000.
- [GKMP98] Dirk Grunwald, Artur Klauser, Srilatha Manne, and Andrew Pleszkun. Confidence estimation for speculation control. In *In 25th Annual International Symposium on Computer Architecture*, pages 122–131, 1998.

- [Hen00] John L. Henning. Spec cpu2000: Measuring cpu performance in the new millennium. *Computer*, 33(7):28–35, 2000.
- [HP03] John L. Hennessy and David A. Patterson. *Computer Architecture, A Quantitative Approach*. Morgan Kaufmann Publishers, San Fransisco, CA, US, 2003.
- [HP08] John L. Hennessy and David A. Patterson. *Computer Organization and Design*. Morgan Kaufmann Publishers, San Fransisco, CA, US, 2008.
- [HPRA02] Christopher J. Hughes, Vijay S. Pai, Parthasarathy Ranganathan, and Sarita V. Adve. Rsim: Simulating shared-memory multiprocessors with ilp processors. *Computer*, 35(2):40–49, 2002.
- [HR07] Andrew D. Hilton and Amir Roth. Ginger: control independence using tag rewriting. In *ISCA '07: Proceedings of the 34th annual international symposium on Computer architecture*, pages 436–447, New York, NY, USA, 2007. ACM.
- [HSF00] Michael Haungs, Phil Sallee, and Matthew Farrens. Branch transition rate: A new metric for improved branch classification analysis. In *In Proc. HPCA*, pages 241–250, 2000.
- [JKL00] Daniel A. Jiménez, Stephen W. Keckler, and Calvin Lin. The impact of delay on the design of branch predictors. In *MICRO 33: Proceedings of the 33rd annual ACM/IEEE international symposium on Microarchitecture*, pages 67–76, New York, NY, USA, 2000. ACM.
- [JL01] Daniel A. Jiménez and Calvin Lin. Dynamic branch prediction with perceptrons. In *HPCA '01: Proceedings of the 7th International Symposium on High-Performance Computer Architecture*, page 197, Washington, DC, USA, 2001. IEEE Computer Society.
- [JRS96] Erik Jacobsen, Eric Rotenberg, and J. E. Smith. Assigning confidence to conditional branch predictions. In *MICRO 29: Proceedings of the 29th annual ACM/IEEE international symposium on Microarchitecture*, pages 142–152, Washington, DC, USA, 1996. IEEE Computer Society.
- [JSHP97] Stéphan Jourdan, Jared Stark, Tse-Hao Hsing, and Yale N. Patt. Recovery requirements of branch prediction storage structures in the presence of mispredicted-path execution. *Int. J. Parallel Program.*, 25(5):363–383, 1997.
- [KG99] Artur Klauser and Dirk Grunwald. Instruction fetch mechanisms for multipath execution processors. In *In MICRO-32*, pages 38–47, 1999.
- [Kop02] David M. Koppelman. The benefit of multiple branch prediction on dynamically scheduled systems. In *Workshop on Duplicating, Deconstructing, and Debunking held in conjunction with the 29th International Symposium on Computer Architecture*, pages 42–51, 2002.

- [Kop08] David M. Koppelman. Lsu ece technical report 2008-dmk-1. Department of Electrical and Computer Engineering, Louisiana State University, 2008.
- [Loh06] G.H. Loh. Revisiting the performance impact of branch predictor latencies. *IEEE International Symposium on Performance Analysis of Systems and Software*, 0:59–69, 2006.
- [LW92] Monica S. Lam and Robert P. Wilson. Limits of control flow on parallelism. *SIGARCH Comput. Archit. News*, 20(2):46–57, 1992.
- [McF93] Scott McFarling. Combining branch predictors. *WRL TN-36*, 1993.
- [MS90] Steven S. Muchnick and Richard Schell. Sun’s compiler technology. pages 69–70, 1990.
- [PSEa] Pse. <http://www.ece.lsu.edu/koppel/pse/>.
- [PSEb] Viewable simulation batch data sets for pse. <http://svn.ece.lsu.edu/ds/cjm/>.
- [PT09] Leo Porter and Dean M. Tullsen. Creating artificial global history to improve branch prediction accuracy. In *ICS ’09: Proceedings of the 23rd international conference on Supercomputing*, pages 266–275, New York, NY, USA, 2009. ACM.
- [RJS99] Eric Rotenberg, Quinn Jacobson, and Jim Smith. A study of control independence in superscalar processors. In *In HPCA-5*, pages 115–124, 1999.
- [RSI] Rsiml. <http://www.ece.lsu.edu/koppel/work/proc.html>.
- [SBV95] Gurindar S. Sohi, Scott E. Breach, and T. N. Vijaykumar. Multiscalar processors. In *In Proceedings of the 22nd Annual International Symposium on Computer Architecture*, pages 414–425, 1995.
- [SI94] CORPORATE SPARC International, Inc. *The SPARC architecture manual (version 9)*. Prentice-Hall, Inc., Upper Saddle River, NJ, USA, 1994.
- [Sit93] Richard L. Sites. Alpha axp architecture. *Commun. ACM*, 36(2):33–44, 1993.
- [SMC00] Kevin Skadron, Margaret Martonosi, and Douglas W. Clark. A taxonomy of branch mispredictions, and alloyed prediction as a robust solution to wrong-history mispredictions. In *In Proceedings of the 2000 International Conference on Parallel Architectures and Compilation Techniques*, page pages, 2000.
- [Smi81] James E. Smith. A study of branch prediction strategies. In *ISCA ’81: Proceedings of the 8th annual symposium on Computer Architecture*, pages 135–148, Los Alamitos, CA, USA, 1981. IEEE Computer Society Press.
- [SPHC02] Timothy Sherwood, Erez Perelman, Greg Hamerly, and Brad Calder. Automatically characterizing large scale program behavior. pages 45–57, 2002.

- [Sto01] Jon Stokes. The pentium 4 and the g4e: an architectural comparison: Part i. <http://arstechnica.com/old/content/2001/05/p4andg4e.ars/4>, 2001.
- [Sto06] Jon Stokes. Into the core: Intel's next-generation microarchitecure. <http://arstechnica.com/hardware/news/2006/04/core.ars/>, 2006.
- [TDF⁺02] J. M. Tendler, J. S. Dodson, J. S. Fields, H. Le, and B. Sinharoy. Power4 system microarchitecture. *IBM J. Res. Dev.*, 46(1):5–25, 2002.
- [yCHyYP94] Po yung Chang, Eric Hao, Tse yu Yeh, and Yale Patt. Branch classification: a new mechanism for improving branch predictor performance. In *In Proceedings of the 27th International Symposium on Microarchitecture*, pages 22–31, 1994.
- [YP92] Tse-Yu Yeh and Yale N. Patt. Alternative implementations of two-level adaptive branch prediction. In *In Proceedings of the 19th Annual International Symposium on Computer Architecture*, pages 124–134, 1992.
- [YP93] Tse-Yu Yeh and Yale N. Patt. A comparison of dynamic branch predictors that use two levels of branch history. In *in Proceedings of the 20th Annual International Symposium on Computer Architecture*, pages 257–266. ACM, 1993.
- [YS99] Cliff Young and Michael D. Smith. Static correlated branch prediction. *ACM Transactions on Programming Languages and Systems*, 21:1028–1075, 1999.

Vita

Christopher J. Michael was born in Kuwait in 1980. His father is of Iraqi-Turkish ethnicity and his mother is of Palestinian-Lebanese ethnicity. He has lived in Baton Rouge, Louisiana since 1982. Among his academic interests are computer architecture, high performance computing, and application development in performance analysis. In the non-academic domain, he enjoys playing his oud and cooking various vegetable, mineral, and animal. He will receive his doctorate in electrical engineering from Louisiana State University in May of 2010. After graduation, he will be conducting post-doctoral research at the Naval Research Lab, Stennis Space Center.